FINITE ELEMENT MODEL FOR PREDICTING RESIDUAL STRESSES IN SHIELDED METAL ARC WELDING OF MILD STEEL PLATES

BY

Ibrahim Ugbede, MUSA

DEPARTMENT OF MECHANICAL ENGINEERING,
FACULTY OF ENGINEERING, AHMADU BELLO UNIVERSITY, ZARIA

OCTOBER, 2015

FINITE ELEMENT MODEL FOR PREDICTING RESIDUAL STRESSES IN SHEILDED METAL ARC WELDING OF MILD STEEL PLATES

BY

Ibrahim Ugbede, MUSA
(MSc/Eng/5900/2011-2012)

A DISERTATION SUBMITTED TO THE SCHOOL OF POSTGRADUATE STUDIES, AHMADU BELLO UNIVERSITY, ZARIA, IN PARTIAL FULFILLMENT OF THE REQUIRMENTS FOR THE AWARD OF THE DEGREE OF MASTER OF SCIENCE (M.Sc) IN PRODUCTION ENGINEERING

DEPARTMENT OF MECHANICAL ENGINEERING,
FACULTY OF ENGINEERING,
AHMADU BELLO UNIVERSITY, ZARIA

OCTOBER, 2015

DECLARATION

I hereby declare that this Thesis entitled "Finite Element Model for Predicting Residual Stresses in Sheilded Manual Metal Arc welding of Mild Steel Plates" was carried out by me in the Department of Mechanical Engineering, and it is a record of my research work. No part of this work has been presented in any previous application for another degree or diploma at any institution. All information obtained from literature have been duly acknowledged in the text and a list of references provided.

_____ _____

Ibrahim Ugbede,MUSA (Student)

Date / Signature

CERTIFICATION

This Thesis, entitled "FINITE ELEMENT MODEL FOR PREDICTING RESIDUAL STRESSES IN SHEILDED MANUAL METAL ARC WELDING OF MILD STEEL PLATES" by Ibrahim UgbedeMUSA, meets the regulations governing the award of the degree of Master of Science (M.Sc) in Production Engineering of Ahmadu Bello University, Zaria, and is approved for its contribution to knowledge and literary presentation.

_____ _____

Dr. M.O. Afolayan Date/ Signature
(Chairman, Supervisory Committee)

_____ _____

Dr. I.M. Dagwa Date/ Signature
(Member, Supervisory Committee)

_____ _____

Dr. M. Dauda Date/ Signature
(Head of Department)

_____ _____

Prof. Kabir BalaDate/ Signature
(Dean, School of Postgraduate Studies)

DEDICATION

This research is dedicated to myMother, Late Mrs Rakiya Abayi Musa

ACKNOWLEDGEMENTS

This thesis would not have been possible without the guidance and the help of several individuals who in one way or another contributed and extended their valuable assistance in its preparation and completion. First and foremost, I would like to express my sincere gratitude to the Chairman of my Supervisory Committee, Dr. M.O. Afolayan, for his continuous support of my M.Sc study and research, for his patience, motivation, enthusiasm and immense knowledge. I could not have imagined having a better supervisor and mentor for my study. In the same vein, I am deeply grateful to Dr I.M. Dagwa, member of the Supervisory Committee,I would like to thank you for encouraging my research and for allowing me to grow as a research scientist. Your advice on both research as well as on my career have been priceless. My supervisors, thank you for your brilliant comments and suggestions.

Besides my Supervisors, I would like to thank the staff of the Department of Mechanical Engineering for their encouragement, insightful comments, and inputs especially Dr. M. Dauda (H.O.D), Prof S.Y. Aku, Prof. A.I. Obi , Dr. D.S. Yawas, Dr. F.O. Anafi, Dr G.Y. Pam, Dr. D.M. Kulla, Engr. Laminu S.K. , Mallam Auwaland all others too numerous to mention. Thank you all.

Apart from my efforts, the success of any project depends largely on the encouragement and guidance of friends. I take this opportunity to express my gratitude to friends Slim, Seedorf, A-tek, Likita, Racheal, Wale, Kenny, Adams, Smokey, Jemima, Dan-j, Soji and to every member of my extended family, I am proud to be of the same blood.

A special thanks to my family. Words cannot express how grateful I am to my father and late mother, Mr. and Mrs. Allan Andrew Musa, for all the sacrifices that you have made on my behalf. Your prayer for me was what sustained me thus far. And to my siblings, Mrs Fatima Opayun (Omeyi), Hauwa Musa (Kuluwa) and Musa J.C. Musa (G-Monee), if I ever have the opportunity of coming back to the world a second time, I will love to still have you as a family.

ABSTRACT

This study investigates the prediction of residual stresses developed in shielded metal arc welding of ASTM A36 mild steel platesvia simulation and experiments. The specific objectives were to simulate the shielded manual metal arc welding process by using the finite element method in ANSYS Multiphysics Version 14, to produce experimental samples of butt welded ASTM A36 mild steel plates, to determine the residual stresses developed in the weldment of the steel plates and those generated from the Finite Element Model Simulation, and to establish correlation between experimental and predicted values of residual stress. Findings indicate that the maximum temperature was 1827°C while that at the end of the plate was maintained at around 27°C. From the Finite Element Model Simulation, the transverse residual stress in the x direction (σ_x) had a maximum value of 375MPa (tensile) and minimum value of -183MPa (compressive) while in the y direction (σ_y), the maximum value of 172MPa (tensile) and minimum value of 0.The longitudinal stress in the x direction (σ_x) indicated a maximum value of 355MPa (tensile) and a minimum value of -10MPa (compressive) while in the y direction (σ_y), the maximum value was 167MPa and the minimum value of the residual stress was -375MPa. The experimental values as measured by the X-Ray diffractometer were similar as transverse residual stress (σ_x) along the weld line in the transverse x directionvaried from 353MPa (tensile) to -209MPa (compressive) while in the y direction, stress (σ_y) along the weld line varied from 177MPa (tensile) to 0. The longitudinal stress measured by the X-Ray diffractometer in the x direction (σ_x) varied from 339MPa (tensile) to 0 (compressive) while in the y direction (σ_y) varied from 171MPa (tensile) to -366MPa (compressive). The result of the correlation coefficient test between the experimental and finite element results of residual stresses the was close to unity (1) which indicates a positive uphill linear relationship. The result of the F-Test conducted was also close to unity (1) which indicates the level of variance between the experimental and finite element results of residual stresses was not significant. Based on these results, it was established that using the 3D FEM analysis, results of residual stresses obtained was in good agreement with the experiment.

TABLE OF CONTENTS

CHAPTER ONE: INTRODUCTION

CHAPTER TWO: LITERATURE REVIEW

CHAPTER THREE: MATERIALS, EQUIPTMENT AND METHODS

CHAPTER FOUR: RESULTS AND DISCUSSION

CHAPTER FIVE: CONCLUSIONS AND RECOMMENDATIONS

LIST OF TABLES

LIST OF FIGURES

CHAPTER 1

INTRODUCTION

1.0 Background of the study

The use of the Finite Element Method (FEM) in product development is now well establishedhowever, its use in manufacturing processes is not very common and is part of the field of new applications in computational mechanics. The most important reason for this development is the industrial need to improve productivity and quality of products and to have better understanding of the influence of different process parameters. The modelled phenomena play an important role at various stages of the production of steel parts, for example, welding, heat treatment and casting, among others.

The importance of these applications lies in determining the evolution of stresses and deformations to predict, for example, susceptibility to cracking and thus prevent failures during manufacturing or even service. Furthermore, this simulation tool can be used to optimize some aspects of the manufacturing process.Welding is defined by the American Welding Society (AWS) as a localized coalescence ofmetals or non-metals produced by either heating of the materials to a suitable temperature with or without the application of pressure, or by the application of pressure alone, with or without the use of filler metal (Mackerle, 2004). Welding techniques are one of the most important and most often used methods for joining pieces in industry. Any information about the shape, size and residual stress of a welded piece is of particular interest to improve quality.

The analysis of welding processes involves several branches of Physics, and requires thecoupling of different models addressed to describe the behaviour of a phenomenological system. Many of these models have been implemented numerically and are being used in an efficient way to solve the problems on an individual basis.

The problem of welding distortion during fabrication processes causes to thedimensional inaccuracies and misalignments of structural members, which can result in corrective tasks or rework when tolerance limits are exceeded. This in turn, increases the production cost and leads to delays. In fabrication and design industries, expenses for rework such as straightening could cost lots of thousands. Therefore, the problems of distortion and residual stresses are always of great concern in welding industry. In order to deal with this problem, it is necessary to define prediction of the amount of distortion resulting from the welding operations. One way to predict the distortion and shrinkage of steel welding is through numerical analysis such as finite element analysis (FEA) (Xu, 2010).

Once the techniques of prediction of the distortion and shrinkage are identified, then theproblems can be controlled accordingly.Within the welding procedures, there are many factors such as welding process type,welding process parameters, welding sequence, preheat patterns, level of constraint and joint details that contribute to the distortion of the welded structure. Knowing which parameters have a major effect on the quality of the weld and which parameters give the most significant effects on the weld quality are the main issues in welding industry. The research activity in welding simulation started decades ago. Rosenthal (1946) was among the first researchers to develop an analytical solution of heat flow during welding based on conduction heat transfer for predicting the shape of the weld pool for two and three dimensional welds. Understanding of the theory of heat flow is essential in order to study the welding process analytically, numerically or experimentally since the pioneering work of Rosenthal (1946), considerable interest in the thermal aspects of welding was expressed by many researchers such as Andrea Capriccioli (2009), and Heinze et al (2012)

1.1 Statement of the Problem

The existence of residual stresses in welded structures has caused fatigue and distortion of machine parts in service and were responsible for failure. These stresses if not properly controlled can lead to the loss of lives and property. Various trial and error welding runs have to be carried out while the welding parameters are varied until optimum conditions are determined. This is wasteful of time, material and finance. Thus the need to incorporate Finite Element Analysis prediction of residual stresses by computational methods to first determine satisfactory welding parameters before actual production is carried out.

1.2 Aim and Objectives

The aim and objectives of this research are briefly highlighted below:

1.2.1 Aim

The Aim of this study is to develop a Finite Element Model for predicting residual stresses in ShieldedMetal Arc Welding of ASTM A36 low Carbon Steel Plates.

1.2.2 Objectives

The Specific objectives of the study are outlined below:

i. To simulate the shielded manual metal arc welding process by usingthe finite element method in ANSYS Multiphysics Version 14 software.
ii. To produce experimental samples of butt welded ASTM A36 mild steel plates.
iii. To determine the residual stresses developed in the weldment of the steel plates and those generated from the Finite Element Model Simulation.
iv. To establish correlation between experimental and predicted values of residual stress.

1.3 Justification

This research is intended to highlight the need for integration of computer aided methods in predicting residual stresses which cause failure during the service of manufactured products. Thus eliminate the waste of time, finance and also save lives. It also aims to minimize production and testing of multiple production setups in other to determine optimum production parameters.

1.4 Scope of Research

The scope of this research would cover ANSYS Multiphysics simulation of the welding process and the corresponding experimental X-Ray diffraction measurement of Residual stresses.

CHAPTER 2

LITERATURE REVIEW

2.0 Introduction

This chapter describes the basic principle and types of welding, residual stresses, finite element modelling of welds, experimental determination of residual stresses anda brief review of other related works.

2.1 Welding

Welding is a process for joining similar metals. Welding joins metals by melting and fusing the base metals being joined and the filler metal applied with or without the application of pressure. Welding employs pinpointed, localized heat input. Most welding involves ferrous-based metals such as steel and stainless steel. Welding covers a temperature range of 1500º F - 3000º F (800ºC - 1635ºC). Welded joints are usually stronger or as strong as the base metals being joined. Welding is used vastly in the manufacturing industry from automobiles, aeronautics, pipelines, shipping and even airspace industry. Electric arc welding, gas welding, resistance welding and energy beam welding are common types of weld processes used in production of welded joints (Radaj, 2003).

2.1.1 TYPES OF ELECTRIC ARC WELDING

This is one of the several fusion processes for joining metals. By applying intense heat, metal at the joint between two parts is melted and caused to intermix directly or more commonly with an intermediate molten filler metal. Some electric arc welding types are Flux-cored arc welding (FCAW), Gas metal arc welding (GMAW), Gas tungsten arc welding (GTAW), Shielded metal arc welding (SMAW). (Howard *et al*, 2006).

2.1.1.1 Flux-cored arc welding (FCAW)

Uses tubular electrodes that are filled with flux. It's much less brittle than the coatings on SMAW electrodes and preserves most of the alloying benefits. The emissive fluxes shield the welding arc from the air, or shielding gases might be used if non-emissive fluxes are required. It's popular when welding heavy sections an inch or more thick thanks to the higher weld-metal deposition rate.

2.1.1.2 Gas metal arc welding (GMAW)

Also known as MIG welding, shields the welding arc with a gas such as argon or helium or even a mixture. Deoxidizers in the electrodes can prevent oxidation which makes it possible to weld multiple layers. It's a simple, versatile, and economical welding process. The temperatures are also relatively low and it is used for thin sheet and sections. It can easily be automated.

2.1.1.3 Gas tungsten arc welding (GTAW)

Is also known as TIG welding. It uses tungsten electrodes as one pole of the arc in order to create the required heat. The gas is argon, helium, or a mixture of those two. Filler wires provide the molten material if it is necessary. This process is good for thin materials and the filler wires are similar in composition to whatever is being welded.

2.1.1.4 Plasma arc welding (PAW)

Have ionized gases and electrodes that generate hot plasma jets that are aimed at the welding area. These jets are extremely hot. The concentration of higher energy is good for narrower and deeper welds as well as an increase in welding speeds.

2.1.1.5 Shielded metal arc welding (SMAW)

This is one of the simplest, oldest, and most versatile welding methods. The arc comes from a coated electrode tip being touched to the workpiece and then withdrawn to maintain the arc. The heat that is generated melts the tip, coating, and base metal and the weld is formed out of that alloy when it solidifies. Slag that is formed and protects the weld from oxides, inclusions, and nitrides has to be removed after every pass. This is commonly used in pipeline work, shipbuilding, and construction.

2.1.1.6 Submerged arc welding (SAW)

Has a granular flux that is fed into the weld zone that forms a thick layer, completely covering the molten zone and preventing sparks and spatter. It allows for deeper heat penetration since it acts like a thermal insulator. The process is limited to horizontal welds and used for high speed sheet or plate steel welding. It can be semiautomatic or automatic. The flux can be recovered and treated then used again. This method provides 4-10 times as much productivity as shielded metal arc welding.

2.1.2 OTHER TYPES OF WELDING

Apart from the electric arc welding, other forms of welding like Oxy-fuel welding, Resistance welding, Spot welding and Energy beam are also used in metal joining processes.

2.1.2.1 Oxy-fuel welding and cutting

The most common gas welding process is oxy-fuel welding, also known as oxyacetylene welding. It is one of the oldest and most versatile welding processes, but in recent years it has become less popular in industrial applications. It is still widely used for welding pipes and tubes, as well as repair work. (American Welding Society, 2001)

2.1.2.2 Resistance welding

Resistance welding involves the generation of heat by passing current through the resistance caused by the contact between two or more metal surfaces. Small pools of molten metal are formed at the weld area as high current (1000–100,000 A) is passed through the metal. In general, resistance welding methods are efficient and cause little pollution, but their applications are somewhat limited and the equipment cost can be high. (American Welding Society, 2001)

2.1.2.3 Spot welding

Spot welding is a popular resistance welding method used to join overlapping metal sheets of up to 3 mm thick. Two electrodes are simultaneously used to clamp the metal sheets together and to pass current through the sheets. The advantages of the method include efficient energy use, limited workpiece deformation, high production rates, easy automation, and no required filler materials. (American Welding Society, 2001)

2.1.2.4 Energy beam

Energy beam welding methods, namely laser beam welding and electron beam welding, are relatively new processes that have become quite popular in high production applications. The two processes are quite similar, differing most notably in their source of power. Laser beam welding employs a highly focused laser beam, while electron beam welding is done in a vacuum and uses an electron beam. (American Welding Society, 2001)

2.2 Residual stresses

Residual stress is defined as “the stress resident inside a component or structure after all applied forces have been removed”.Compressiveresidual stress acts by pushing the

material together, while tensileresidual stress pulls the material apart. Stresses can also be characterized as normal stresses that act perpendicular to the face of a material and shear stresses that act parallel to the face of a material. There are a total of 6 independent stresses at any point inside a material represented by $\sigma_{ij}$where i is the direction that the stress is acting and j is the face the stress is acting on.

2.2.1 Causes of Residual Stress

Residual stresses are generated, upon equilibrium of material, after plastic deformation that is caused by applied mechanical loads, thermal loads or phase changes. Mechanical and thermal processes applied to a component during service may also alter its residual stress state (Cook, 1995).

2.2.2 Types of Residual Stress

Residual stresses can be characterized by the scale at which they exist within a material. Stresses that occur over long distances within a material are referred to as macro-stresses. Stresses that exist only locally (either between grains or inside a grain) are called micro-stresses. The total residual stress at a given location inside a material is the sum of all 3 types of stresses (Abu, 2013).

i. Type I Stresses: Macro-stresses occurring over distances that involve many grains within a material.
ii. Type II Stresses: Micro-stresses caused by differences in the microstructure of a material and occur over distances comparable to the size of the grain in the material. Can occur in single-phase materials due to the anisotropic behaviour of individual grains, or can occur in multi-phase material due to the presence of different phases.

iii. Type III Stresses: Exist inside a grain as a result of crystal imperfections within the grain.

2.2.3 Effects of Residual Stress

Residual stress effects are the following; distortion, crack initiation and propagation,peen forming (controlled distortion), fretting, stress corrosion cracking (SCC) and hydrogen initiated cracking (HIC).

2.2.3.1 Distortion

Welding distortion is defined as the non-uniform expansion and contraction of weld metal and adjacent base metal during the heating and cooling cycle of the welding process. Distortion is a consideration when arc welding all materials and the principles behind this reaction are fundamentally the same. The non-uniform heating, resulting in non-uniform expansion and contraction, along with weld metal and base metal shrinkage and the partial restraint from the less affected parts of the structure, are the primary causes of thermal distortion problems in welding(Dean and Hidekazu,2008).

2.2.3.2 Crack initiation and propagation (Damage tolerance)

Fatigue is the weakening of a material caused by repeatedly applied loads. It is the progressive and localized structural damage that occurs when a material is subjected to cyclic loading.Fatigue occurs when a material is subjected to repeated loading and unloading. If the loads are above a certain threshold, microscopic cracks will begin to form at the stress concentrators such as the surface, persistent slip bands (PSBs), and grain interfaces. Eventually a crack will reach a critical size, the crack will propagate suddenly, and the structure will fracture(American metallurgical consultants,2012).

2.2.3.3 Peen forming (controlled distortion)

Is a cold working process used to produce a compressive residual stress layer and modify mechanical properties of metals. It entails impacting a surface with shot (round metallic, glass, or ceramic particles) with force sufficient to create plastic deformation. The mechanical working of metals by means of hammer blows. Peening tends to stretch the surface of the cold metal, thereby relieving contraction stresses (Curtis-Wright Corporation, 2009).

2.2.3.4 Fretting

Fretting corrosion has been the cause of countless failures at the contact points of machinery components.Fretting is a special wear process that occurs at the contact area between two materials under load and subject to minute relative motion by vibration or some other force.When two pieces of material, pressed together by an external static load, (for example, bolted flanges, riveted lap-joints, press-fits such as a gear or bearing on a shaft) are subjected to a transverse cyclic loading, so that one contacting face is relatively displaced cyclically parallel to the other face, in the presence of high contact stress, wear on the mating surfaces occurs. If the magnitude of the displacement is less than about 0.003 inches, the wear is termed "fretting" (American metallurgical consultants,2012).

2.2.3.5 Stress corrosion cracking (SCC) and hydrogen initiated cracking (HIC)

Stress corrosion cracking is a progressive fracturing that occurs in metals as a result of the combined influence of tensile stress and a corrosive environment. Structural failure due to corrosion cracking is often sudden and unpredictable, occurring after as little as a few hours of exposure, or after months or even years of satisfactory service. Metal components frequently experience SCC and HIC; virtually all alloy systems are susceptible to corrosion cracking by a specific corrodent under a specific set of conditions(Naeem, 2009).

2.3 Finite Element Model

The finite element method (FEM) is a computational technique used to obtain approximate solutions of boundary value problems in engineering. The finite element method is a way of getting a numerical answer to a specific problem. A simple description of FEM is the cutting of a structure into several elements, describing the behaviour of each element in a simple way, reconnecting the elements at ”nodes” as if it were pins or drops of glue that held the elements together. (David, 2001)

2.3.1 Finite Element Analysis of Welding

The numerical modelling of welding can be used as design tool or manufacturing analysis tool. As a design tool, FEM can be used to evaluate the feasibility of designs as early as the concept phase. As a manufacturing analysis tool, for fixed designs, different welding processes and sequences can be evaluated to minimize welding distortion (Michelaris, 1996).

Other parameters that are also involved in the FEA of welding is temperature and history dependent material properties, high gradients of temperature, stress and strain fields with respect to both time and spatial coordinates, large deformations in thin structures, phase transformation and creep phenomena.Firstly the computation of the temperature history during welding and subsequent cooling would be completed and this temperature field would be applied to the mechanical model as a body force (load) to perform the residual stress analysis. To simulate the moving heat source it is necessary to model the heat source during each time increment. In this analysis the moving heat source is simplified by assuming that the welding arc stayed at an element with constant specific volume heat flux, and then moved to the next element at the end of the load step as the welding is finished.

The governing equation for transient heat transfer during welding process analysis is given by equation 2.1 (Goldak et al, 1984).

$$\rho c \frac{\partial T}{\partial t}(x, y, z, t) = \nabla . q(x, y, x, t) + Q(x, y, x, t) 2.1$$

Where

ρ is the density (kg m^{-3}) of the material,

C is the specific heat capacity (J kg^{-1} K^{-1}),

T is the current temperature,

q is the vector of heat flux,

Q is the rate of internal heat generation (W m^{-3}),

t is the time (s),

∇ is the spatial gradient operator and x, y, z are the coordinates in the reference plane.

The non-liner isotropic Fourier heat flux constitutive equation given byEq. 2.2 is employed.(Goldak et al, 1984)

$$q = -k\nabla T 2.2$$

Where

k (W m^{-1} K^{-1}) is the temperature dependent thermal conductivity.

The most widely acceptable double ellipsoidal heat source model, presented by Goldak et al. as shown in Figure 2.1, is used to present the heat generated by the welding torch for the heat input distribution to the weld.

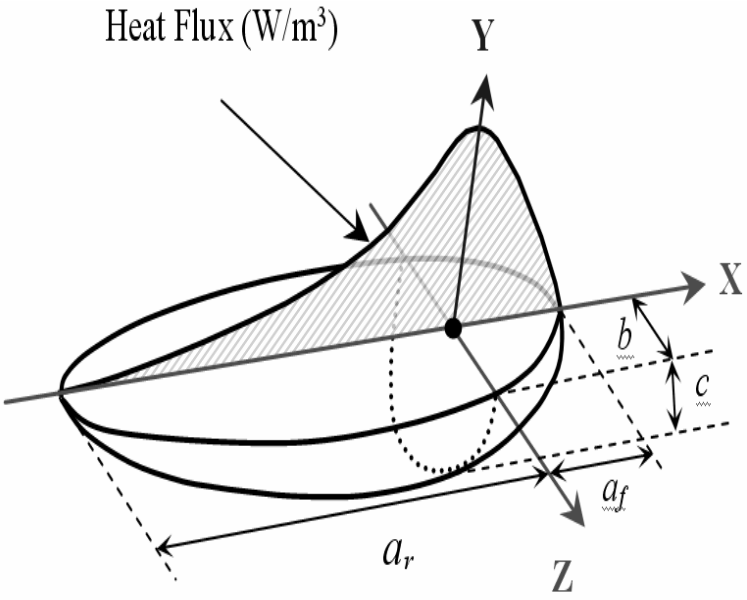

Figure 2.1 Heat source model used in the present study (Goldak et al,1986)

The spatial heat distribution in a moving frame of reference can be calculated with the governing equations 2.3 and 2.4 (Goldak et al, 1984).

$$q_f = \frac{6\sqrt{3}\eta Q f_f}{\pi\sqrt{\pi} a_f bc} e^{\left(-3\left(\frac{x^2}{a_f{}^2}+\frac{y^2}{b^2}+\frac{z^2}{c^2}\right)\right)} \quad 2.3$$

$$q_r = \frac{6\sqrt{3}\eta Q f_f}{\pi\sqrt{\pi} a_r bc} e^{\left(-3\left(\frac{x^2}{a_f{}^2}+\frac{y^2}{b^2}+\frac{z^2}{c^2}\right)\right)} \quad 2.4$$

Where

$Q = VI$ and $ff + fr = 2$,

af is the length of the front ellipsoidal (m),

ar is the length of rear ellipsoidal (m),

b is the width of heat source (m),

c is the depth of heat source (m),

ff is the fraction of heat in front ellipsoidal,

fr is the fraction of heat in rear ellipsoidal,

Q is the total heat input (watts),

V is the welding voltage (volts),

I is the welding current (amperes)

The calculated volumetric heat flux densities are assigned to specific elements around the welding areas in the FE model to simulate the welding torch movement with the specific welding speed.

After the finite element model is developed, the movement of the electrode is simulated using the birth and death of element technique. The technique implies that birth of an element takes place when heat is applied to the element. Element is active until the temperature is dissipated to the surrounding through conduction, convection and radiation. Death of element occurs when heat dissipation ends and temperature of element reaches the ambient temperature. (Stamenkovic and Ivana,2009)

The same welding parameters used in the experimental setup were used in the ANSYS analysis.

The temperature history of each node from the preceeding thermal analysis is input as nodal body load in conjunction with temperature-dependent mechanical properties and structural boundary condition. Thermo-elastic–plastic material formulation as shown by Equation 2.5 with Von-Mises yield criteria is employed with σ_1, σ_2, and $\sigma_3$being the three principal stresses, coupled to a kinematic hardening rule.

$$\sigma_v = \sqrt{\frac{1}{2}[\,(\sigma_1 - \sigma_2)^2 + (\sigma_2 - \sigma_3)^2 + (\sigma_3 - \sigma_1)^2]} \qquad 2.5$$

Same meshing parameters from thermal analysis were used to facilitate the nodal data mapping and elements with same topology to enhance convergence during the

structural analysis.In structural analysis, the only boundary condition is the constraints applied to represent the clamping of the plates to be welded in welding positioners, i.e., all the nodes at the positioned end of the plates, on a Cartesian coordinate axis, are constrained in axial direction.

2.3.2 Two-dimensional vs. Three-dimensional Modelling

A full three-dimensional model with a sufficiently fine mesh can model the heat flow as accurately as the errors in the material properties, geometry, heat input, convection and radiation parameters permit (Cronje, 2005). The reason that three-dimensional analysis has not been standard procedure for the thermal analysis of welds is that it is time consuming and resource intensive.

In choosing proper models for weld analysis, the analyst must balance accuracy against cost. In two-dimensional (2D) cross-sectional models as seen in Figure 2.2, heat flow is constrained in the plane of the plate. These 2D models can achieve accurate results for thin plates. Assuming heat transfer only in the cross-sectional plane can provide a useful and economical approximation for many welding situations.

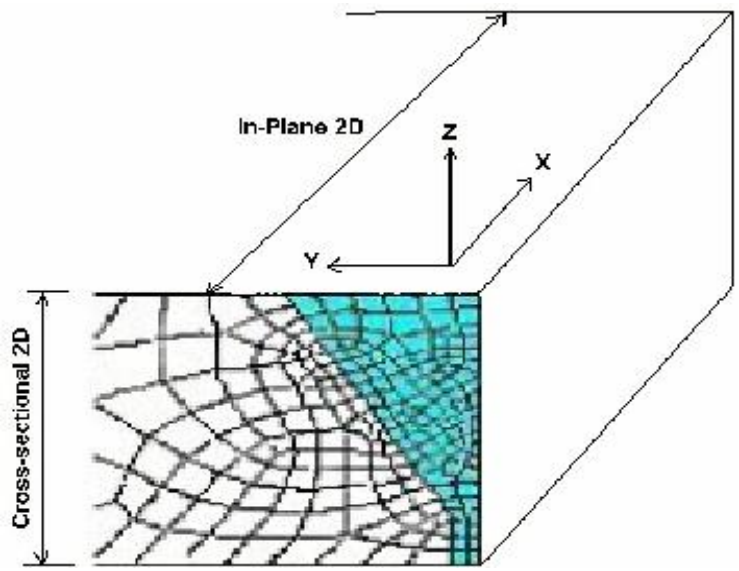

Figure2.2:Illustration of the 2D and 3D planes in the modelling of welded plates (Cronje 2005)

Cross-sectional 2D offers accurate results for predicting residual stresses. Large structures may buckle due to residual stresses parallel to the welding direction. These 2D models cannot represent buckling caused by longitudinal stresses. A fully three-dimensional thermo-mechanical simulation of a large structure can represent this distortion mode (Bonifaz, 2000).

Earlier studies on weld response were limited to cross-sectional 2D modelling. Studies had shown that good correlations were observed between numerical predictions and experimental results for these models. Residual stress predictions in 2D modelling provided accurate estimations comparable to 3D analyses, since the stress field exhibits a uniform distribution through the length of the work piece (Deo *et al*, 2002).

2.3.3 Finite Element Analysis Type

The butt-weld joint of two low carbon steel ASTM A36 plates were modelled using ANSYS Multiphysics V14. To simplify the welding simulation, an un coupled thermo-mechanical analysis would be carried out. Therefore the thermal and mechanical analysis were performed separately. The result of the thermal analysis would be applied as a heat load to during the structural analysis to complete the solution of the Finite element model (Abu, 2003)

ANSYS Multiphysics V14is commercially available engineering software which can be used to model and simulate various engineering processes. It has vastly been applied in thermodynamics, fluid mechanics, electromagnetic and structural engineering capacities. For this research, ANSYS Multi-physics V 14 was used. This is because of its availability, user friendly analysis environment, capacity to carry out a wide range of simulations and analysis, it is relatively cheap and the availability of a large data resource from experts in this field.

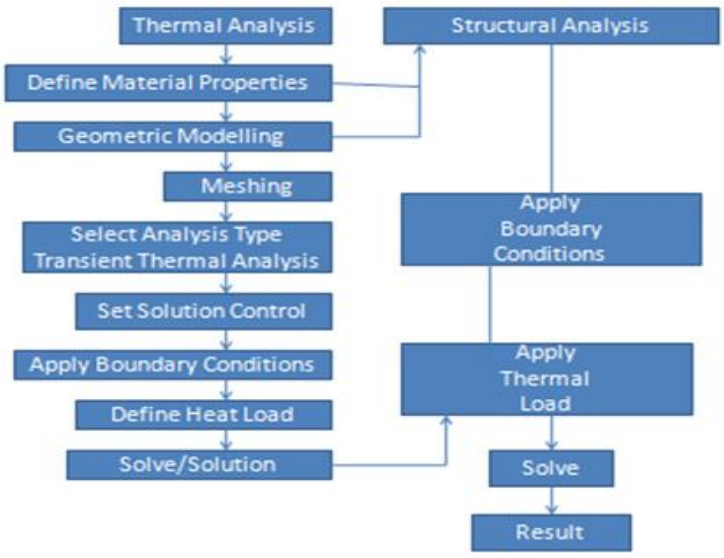

Figure 2.3: Flow chart of uncoupled thermo-mechanical Finite element analysis

2.3.3.1 Thermal Analysis.

Thermal analysis helps understand how the material would behave under temperature dynamics. Transient thermal analysis was used as it determines the temperature values from the transient analysis as a result of the heat flux input.

i. ***Defining Element type***

The element type used for the model was SOLID70. It has a 3-D thermal conduction capability. The element has eight nodes with a single degree of freedom-temperature, at each node. The element is applicable to a 3-D, steady-state or transient thermal analysis. The element also can compensate for mass transport heat flow from a constant velocity field (Nguyen, 2004).

The geometry of solid 70 element type is shown in Figure 2.4

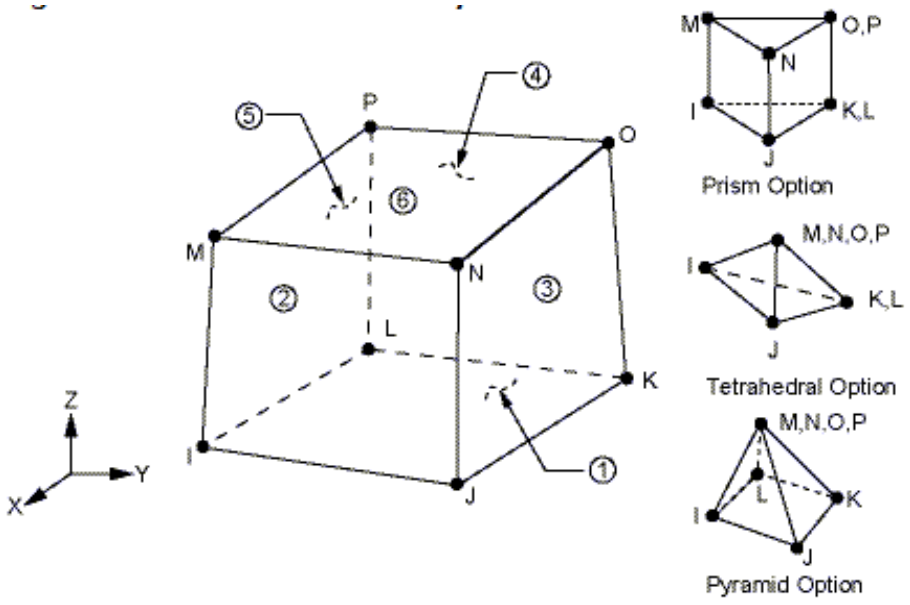

Figure 2.4: Solid 70 Element Type Geometry

This element type is auto assigned for thermal analysis by the ANSYS Multiphysics software V14 but manually assigned in ANSYS Mechanical or lower versions of the software.

ii. ***Defining material properties***

There were several thermal properties required to be applied on the model. These properties were inserted based on the metal plate properties, ASTM 36 low carbon steel used for the experimental procedure. The properties needed were thermal conductivity, specific heat and density (David, 2001). These properties change with temperature.

The material properties as assigned on the materials property interface in ANSYS Multiphysics is shown in Figure 2.5

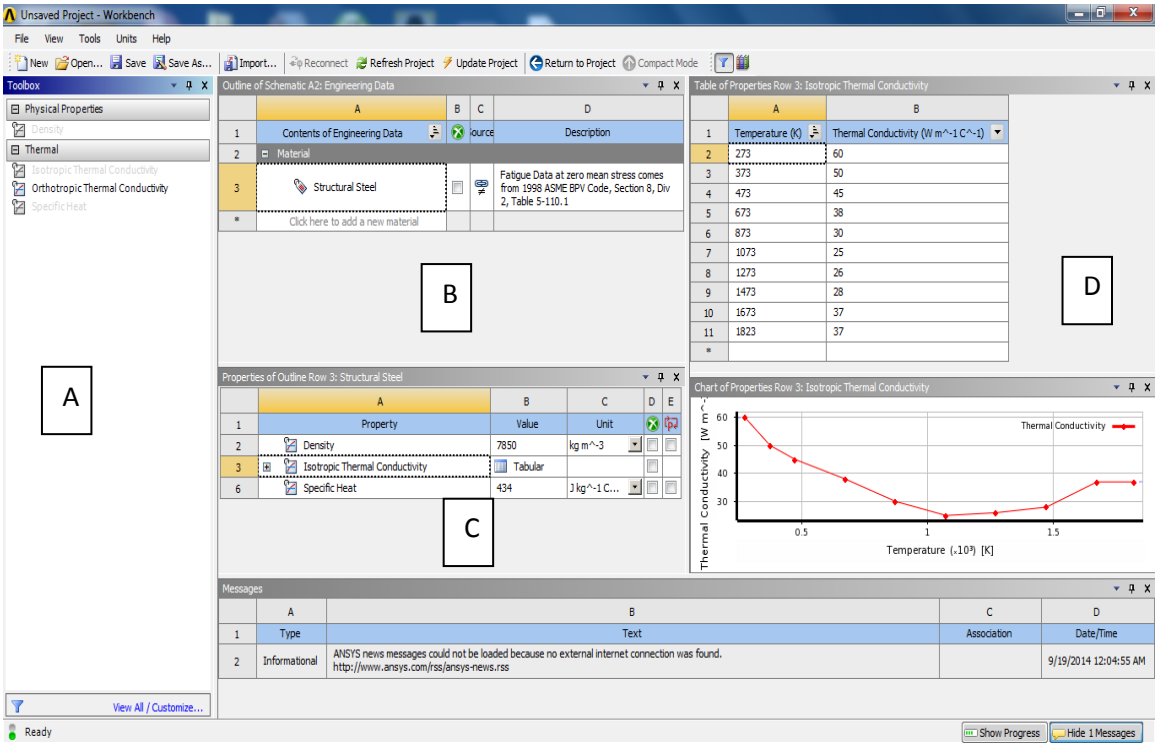

Figure 2.5: Material properties of the steel plates used in the thermal analysis (ANSYS Multiphysics V14)

Area A describes the main menu were material properties are assigned. Area B shows where various engineering material can be selected e.g. structural steel, Aluminium Alloy, concrete, Air e.t.c. Area C represents where the material properties are presented.

Area D shows where the values of the material properties as they change with temperature are imputed.

iii. ***Modelling Assumptions***

a) The Material properties of the filler and electrode and the same as that of the base metal. This is done so that the same chemical and mechanical properties apply to both the filler and parent metal. This ensures a simplification of the Finite Element Model Simulation (Abu, 2013).

b) The Mechanical properties are time dependant, they change as time progresses. Chang and Teng (2004) noted that when the temperature increases, the modulus of elasticity, yield stress, and thermal conductivity for ASTM A36 carbon steel decreases and vice versa.

c) The analysis was based on quasi-steady state where the heat source was moving at a constant velocity. Thus ensuring that the welding simulation would be completed at the specified time.

d) Temperature distribution along the element was constant at all surfaces of the element.

e) Heat input was at a constant speed of 2mm/sec. This replicates the speed at which the electrode would travel during the weld.

f) Convection boundary condition was applied on the model.

g) Radiation heat transfer was neglected. As this would have little effect even on the actual experimental welding process.

h) Initial temperature was set to 27^{o}C.Which is the expected room temperature at which the welding process would be started.

i) Electrode diameter was also assumed to be 3.142mm.

iv. ***Boundary Conditions***

a) The bulk air temperature was 27^{o}C.

b) Convection heat transfer was applied on the model based on equation 2.6

$$Q = h_c A (T\text{-}T_A) \qquad 2.6$$

Where h_c=15 $\frac{W}{m^2}{}^{o}$C

c) Estimation connection heat transfer coefficient, for carbon steel was set to15W/ (m^{2o}C).

v. ***Geometrical Modelling***

The geometry of the model in which the residual stress is to be simulated was created in ANSYS Multiphysics V14 design modeller. Three volumes were created for the model. The first and third volume are the (metal plates) and the second was the filler metal. The dimensions of the model are 6mm (thickness), 100mm (width) and 200mm (length).

The geometry of the created volumes is shown in Figure 2.6

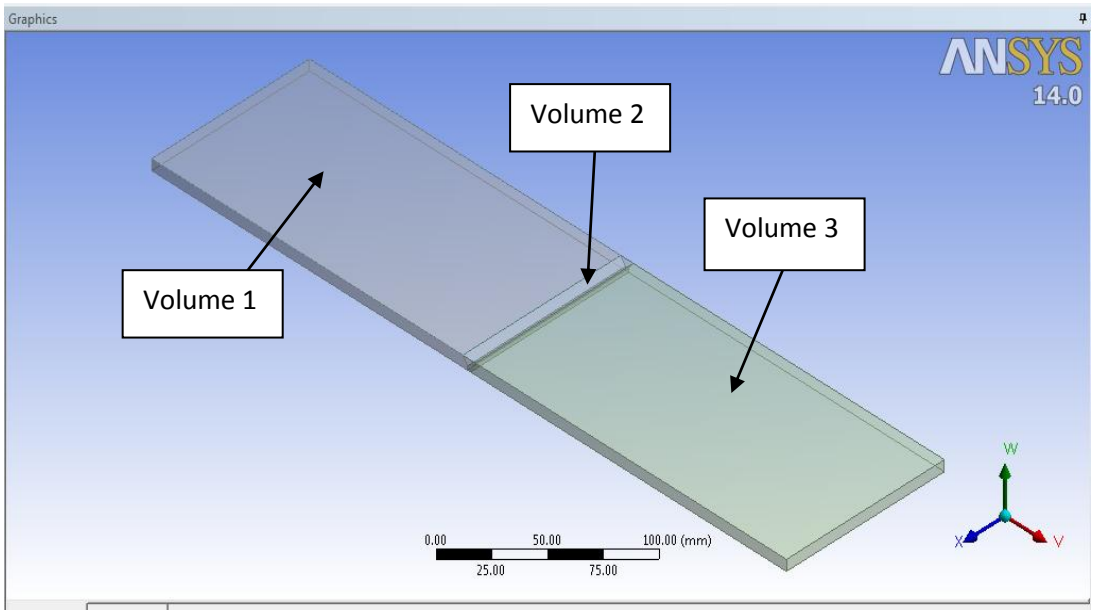

Figure 2.6: Model of the steel welded plates (ANSYS Multiphysics V14)

vi. ***Meshing***

Meshing is a method in which the model is sub divided into small pieces of simple shapes (elements) connected at common points (nodes). The automatic mesher in the software generates a mesh based on a global element size, tolerance, and local mesh control specifications. The size of the mesh depends on the analysis type. Meshing generates 3D tetrahedral solid elements, 2D triangular shell elements and 1D beam elements. A mesh usually consists of one type of element unless the mixed mesh type is specified.

The generated mesh is shown in Figure 2.7

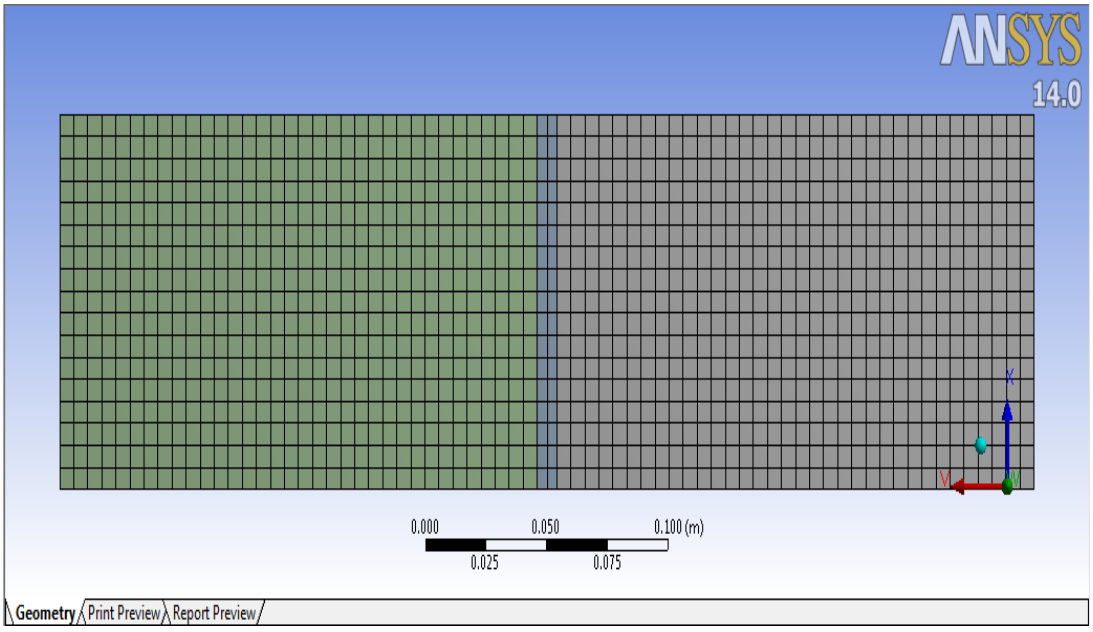

Figure 2.7: Meshed model of steel plates (ANSYS Multiphysics V14)

The properties of the mesh as used in the Analysis are shown in Table 2.1

Table 2.1: Properties of the Mesh

Property	Value
Element Size	Default
Smoothing	Medium
Transition	Fast
Span Angle	Fine
Shape Checking	Standard Mechanical
Nodes	14073
Elements	2380

vii. ***Defining the Heat load input to the model***

Heat input during welding simulation was modelled by a distributed heat flux applied on the individual elements. The heat was applied through birth and death technique. The birth and death technique was used to deactivate and reactivate selected elements thus simulating filler material deposition in the welding process. When an element is deactivated or killed, its stiffness, mass, element loads have a zero value and when an element is activated its stiffness, mass, element loads return to their full original value (Fanous *et al*, 2003). Heat input is that which is obtained from the experimental process and based on equation 2.7 (Bonifaz, 2000).

$$Q = \frac{\eta VI}{vx} \quad 2.7$$

where

η = Arc efficiency

V = Arc voltage (V)

I = Current (I)

υ = Travel speed (mm/s)

x = Electrode diameter (mm)

Similar to the experiment, the weld parameters were:η = 0.75, V= 25V, I = 90A, $\upsilon = 2(mm/s)$, x = 3.142mm.

2.3.3.2 Structural Analysis

The structural analysis was conducted to determine the effects of thermal loads on the physical structure of the metal.Structural properties of the metal such as yield strength, tensile strength, poison ratio, young modulus and melting point are required for the complete structural analysis. The geometry and meshing are the same as used in the thermal analysis.

i. ***Change element***

The element type SOLID70 which was used for the transient thermal analysis would be replaced with SOLID 185. SOLID185 is used for 3-D modeling of solid structures. It is defined by eight nodes having three degrees of freedom at each node: translations in the nodal x, y, and z directions. The element has plasticity, hyperelasticity, stress stiffening, creep, large deflection, and large strain capabilities. It also has mixed formulation capability for simulating deformations of nearly incompressible elastoplastic materials, and fully incompressible hyperelastic materials.

The geometry of SOLID 185 element type is shown in Figure 2.8

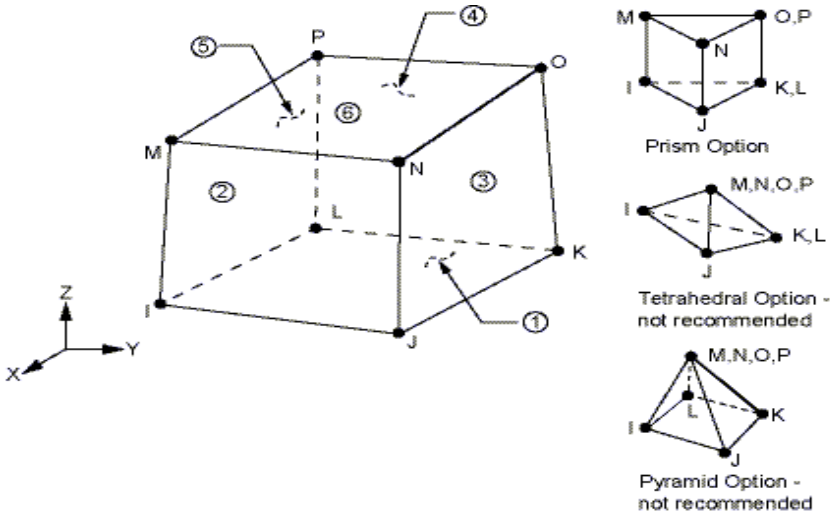

Figure 2.8: Solid 185 Element type Geometry

GUI method: ANSYS main menu > pre-processor > element type > switch Elem Type

The computational interface is shown in Figure 2.9

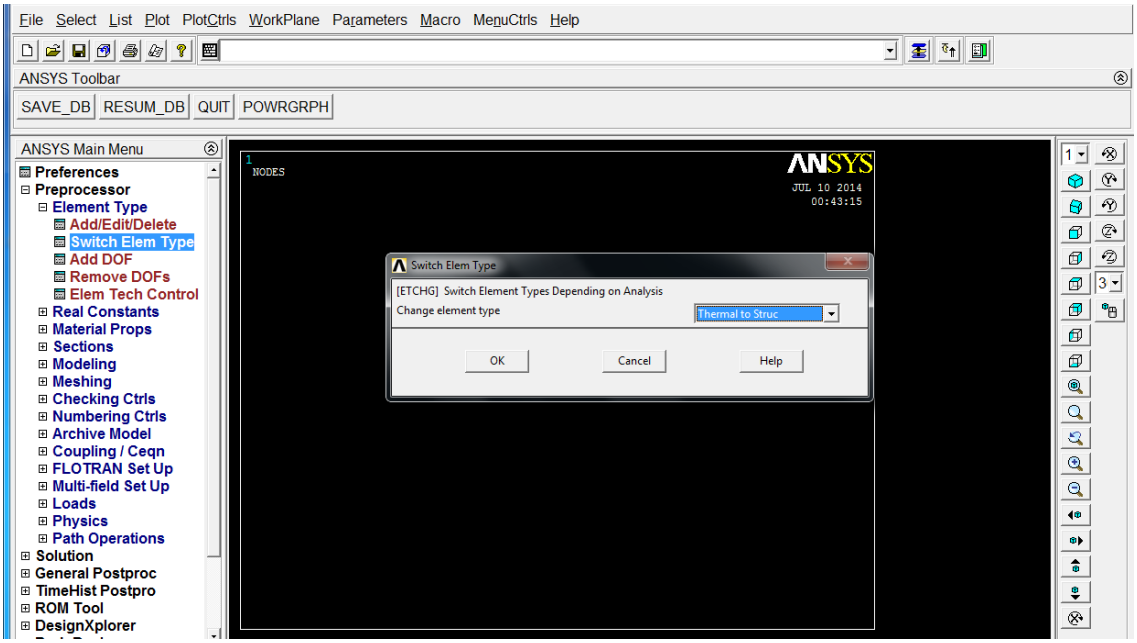

Figure 2.9: Switching the element type of the model

ii. ***Definition of Material Properties***

The structural properties were defined to perform the structural analysis. These include yield strength, tensile strength, poison ratio, young modulus as detailed in table

3.1. These properties ensure that ANSYS Multiphysics software would efficiently model any structural change undergone during the welding simulation process. This includes but not limited to Deformation, Strains and stresses.

GUI method: ANSYS main menu > pre-processor > material props > materials models.

iii. ***Specifying initial Conditions***

Both ends of the plates were assumed to be clamped and the displacement was fixed to be zero at both ends of the plates

a) Displacement

GUI method: ANSYS main menu > pre-processor > loads > Apply > structural Displacement > On Nodes

b) Reference temperature

GUI method: ANSYS main menu > solution > Define loads > settings > Reference Temp

c) The work piece was clamped at both ends during the actual welding process so for the structural analysis, they were subjected to constraints at the left and right side area.

2.4 Experimental process

The experimental process covers the actual welding of the specimen using shielded metal arc equipment and electrodes, the geometry of the weld specimen and the measurement of residual stresses generated during the weld.

2.4.1 Experimental preparation of Specimen

2.4.1.1 Shielded metal arc Welding

Shielded metal arc welding equipment typically consists of a constant current welding power supply and an electrode, with an electrode holder, a ground clamp, and welding cables (also known as welding leads) connecting the two. The power supply used in SMAW has constant current output, ensuring that the current (and thus the heat) remains relatively constant, even if the arc distance and voltage change. This is important because most applications of SMAW are manual.The preferred polarity of the SMAW system depends primarily upon the electrode being used and the desired properties of the weld. Direct current with a negatively charged electrode (DCEN) causes heat to build up on the electrode, increasing the electrode melting rate and decreasing the depth of the weld. Reversing the polarity so that the electrode is positively charged (DCEP) and the workpiece is negatively charged increases the weld penetration. With alternating current the polarity changes over 100 times per second, creating an even heat distribution and providing a balance between electrode melting rate and penetration (Goodheart-Willcox Co., Inc, 2011).

Typically, the equipment used for SMAW consists of a step-down transformer and for direct current models a rectifier, which converts alternating current into direct current. Because the power normally supplied to the welding machine is high-voltage alternating current, the welding transformer is used to reduce the voltage and increase the current. As a result, instead of 220 V at 50 A, the power supplied by the transformer is around 17–45 V at currents up to 600 A.

Other parts of the Shielded manual metal arc welding machine are :

i. Welding Leads: The electrical cable that connects the electrodeholder to a welding machine is the electrode lead. Theworkpiecelead(ground) is the electrical cable thatconnects the base metal to the welding machine.On large welding machines, leads may berequired to carry 600A or more. Leads must have alarge diameter to carry such high current. They mustalso be flexible so a welder can easily move them.

ii. Lead Connections: Welding leads are connected to the welding machine and base metal with lugs, clamps, or special terminals.

iii. Electrode Holder: The electrode holder is held by the welder during the welding operation. The well-insulated handle of the electrode holder protects the welder from electrical shock. An electrode is clamped in the copper alloy jaws of the electrode holder. The jaws provide a good electrical contact for the electrode. The electrode lead is clamped into the electrode holder and the cable clamp is under the insulated handle.

iv. Protective Clothing: These include coveralls, boots, glasses, rubber gloves, welding helmets, lenses. To prevent the occurrence of accidents during welding.

v. Work Booth and Table: The welding table is part of the arc welding station. The workpiece lead may be bolted to the table with a lug or attached to the table with a spring clamp. A weld positioner may be welded or clamped to the table. Welding may be done in a work boothor in an open area.

A schematic representation of the Shielded manual metal arc electrode is shown in Figure 2.10

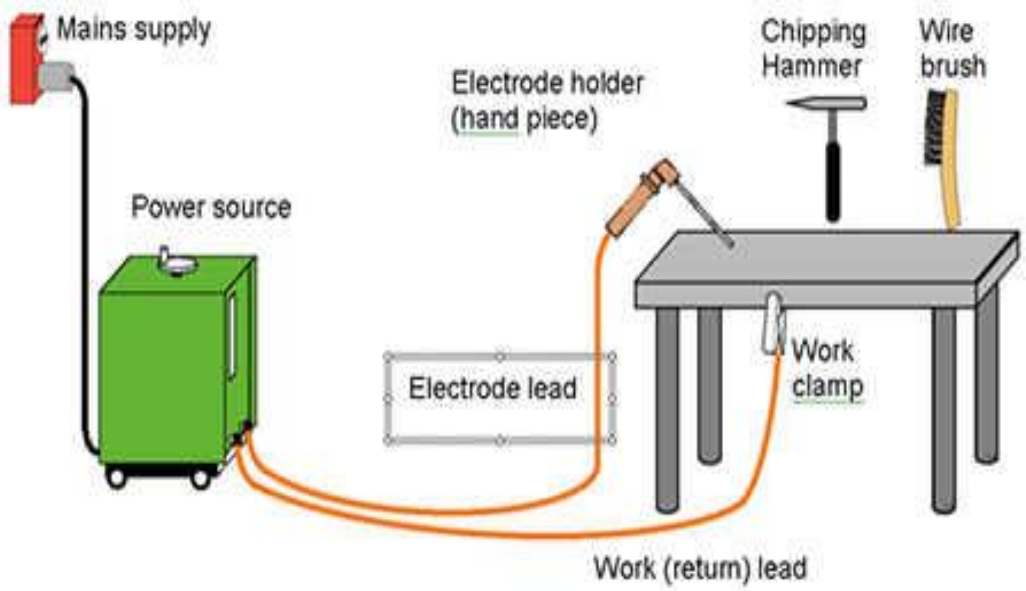

Figure 2.10: Shielded manual metal arc welding machine

(Source: www.weldingweb.com/smmawm/pic.htmlaccessed on 25th august, 2015)

2.4.1.2 Filler Metal (electrode)

An electrode is a tool used in arc welding to produce electric arc. It may be used as a positively charged anode or as a negatively charged cathode. Welding electrodes are made of an electrically conductive material and conduct electric current to the weld. Electrodes may be consumable or nonconsumable. Consumable electrodes include welding wires, rods, plates, and strips with a solid cross section, wires and tapes with powdered cores and covered or combination electrodes (fusible tips). Nonconsumable electrodes include rods and electrodes used in resistance welding. Consumable electrodes also provide the filler metal of the weld puddle. The use of consumable electrodes of appropriate composition makes it possible to change the composition of the weld, alloy the weld with specific components, and lower the content of undesirable impurities. Depending on their purpose, consumable electrodes may be made of a variety of metals or alloys, including steel, aluminium, titanium, and copper.

A covered electrode consists of a rod and a covering. The rod may be fabricated from welding wire, or it may be cast. The covering is made from a mixture of materials that promote the ionization of the atmosphere near the welding arc, provide shielding against the undesirable effects of the atmosphere, and are effective in the metallurgical treatment of the melt puddle. Powder-filled tubes and strips consist of a metal shell filled with a powdered substance. Such substances include gas-forming and slag-forming materials, ferrous alloys, and metals (American Welding Society, 2001)..

E6011 which was used in this research is a high-cellulose potassium electrode designed to be used with AC current. This electrode is used for all-position AC welding and for welding on rusty, dirty, less-than-new metal. It has a deep, penetrating arc and is often the first choice for repair or maintenance work when DC is unavailable. It is commonly used for welding mild steels such as ASTM A-36, A-283, A-284, A-285, A-515, and A-516. Typical applications are railroad cars, truck frames, storage tanks, bridges, boilers, barges and ships (www.onealsteel.com/carbon-steel-plate-a36.html, accessed on 19th January,2014).

Available Diameters: 2.5 mm, 3.2 mm, 4.0 mm, and 5.0 mm

Recommended Operating Current Ranges:

2.5 mm: 65 ~ 90 Amps
3.2 mm: 80 ~ 120 Amps
4.0 mm: 130 ~ 170 Amps
5.0 mm: 170 ~ 210 Amps

These electrodes are readily available for commercial use and are relatively cheap. Some of the E6011 electrodes that were used in welding the ASTM A36 low carbon steel plates are shown in Figure 2.11

Figure 2.11: E6011 Electrodes (Source: Gorgeous metal makers limited)

2.4.1.3 Wire Brush

This is a tool usually made of a handle (wooden or plastic) and a brush. The brush is made of a large number of steel wire bristles. It was used for cleaning the welding surface, to remove carbon deposit on the welded surface, removal of slag in order to expose the actual heat affected zone for effective measurement of the residual stresses developed during the welding.

2.4.1.4 Clamps

Two G-clamps were used to hold the steel plates rigidly during the welding process. This is to ensure that no distortion of the weld specimen occurred after the welding had been completed. The clamps were placed at the edge of the steel plates, farthest away from the weld center line to ensure minimal loss of heat due to conduction from the steel plates through the clamps.

2.1.4.5 Nitric Acid solution

A solution of nitric acid (10% nitric acid and 90% water) by volume is an oxidizing agent which is used to degrease and wash the surface of the welded joint and remove all slag inclusions after treating with a wire brush.

2.1.4.6 XMAS 2.0 Software

This software was used to analyse the result obtained from the x-ray diffraction procedure and thus characterizes the d-spacing, the resulting shift in lattice spacing, the developed strain and also computation of the generated residual stresses from the welding process.

2.4.1.7 Experimental Specimen

The specimen that was used for the experimental process were two steel plates of (low carbon steel – ASTM A36). It is the most commonly used mild and hot-rolled steel. It has excellent welding properties and is suitable for grinding, punching, tapping, drilling and machining processes (Jeyakumar et al, 2013)

The elemental composition of ASTM A36 Low Carbon Steel is shown in Table 2.2

Table 2.2 Elemental Composition of ASTM A36 Low Carbon Steel

Element	**Content %**
Carbon, C	0.25-0.290
Copper, Cu	0.20
Iron, Fe	98.0
Manganese, Mn	1.03
Phosphorous, P	0.040
Silicon, Si	0.280

Also, the material properties are shown in Table 3.2. These properties vary with temperature during mechanical operations like welding, smelting, forging e.t.c. This was taken into consideration in this work. ASTM A36 steel exhibits good strength coupled with formability. It is easy to machine and fabricate and can be securely welded. The machinability rate of ASTM A36 is estimated to be 72%, and the average surface cutting feed of ASTM A36 is 120 ft/min. (www.onealsteel.com/carbon-steel-plate-a36.html)

Table 2.3: Material properties of ASTM A36 (Dean and Hidekazu, 2008)

No	**Temperature (k)**	**Specific heat (j/kg.k)**	**Conductivity (w/m.k)**	**Yield stress (mpa)**	**Thermal Expansion Coeff. (10^{-5}/k)**	**Young's Modulus (gpa)**
1	273	480	60	380	1.1	210
2	373	500	50	340	1.15	200
3	473	520	45	315	1.2	200
4	673	650	38	230	1.3	170
5	873	750	30	110	1.42	80
6	1073	1000	25	30	1.45	35
7	1273	1200	26	25	1.45	20
8	1473	1400	28	20	1.45	15
9	1673	1600	37	18	1.45	10
10	1823	1700	37	15	1.45	10

2.4.1.8 Weld Specimen Geometry

The geometry of the steel plate was 6 mm thick and 100 mm wide (along the welding direction) and 200 mm in the transverse direction. The weld-groove angle was 60°

with a 2mm root opening as shown in Figure 2.12. This less complex geometry was adopted in other to simplify the finite element simulation of the welding process.

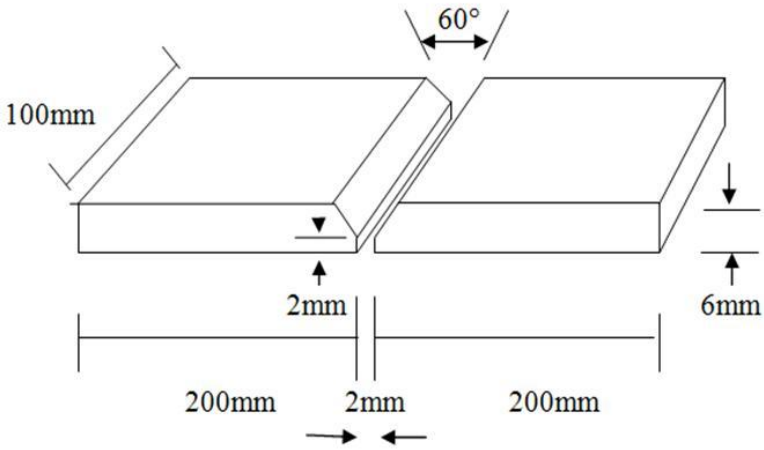

Figure 2.12: Butt weld specimen geometry

2.4.2 Experimental Measurement of Residual Stress

There are various experimental methods of measuring residual stresses. Some are destructive methods which can involve permanent or temporary damage to the specimen. The other methods are classified as non destructive since the specimen is usually not physically damaged.

2.4.2.1X-Ray Diffraction Technique

The x-ray diffraction (XRD) technique exploits the fact that when a metal is under Stress (applied or residual), the resulting elastic strains can cause the atomic planes in the metallic crystal structure to change their spacing. Since metals are composed of atoms arranged in a regular three-dimensional array to form a crystal, most metal components of practical interest consist of many tiny crystallites or grains that are randomly oriented with respect to their crystalline arrangement, and are fused together to make a bulk solid.

When such a polycrystalline metal is subjected to stresses, elastic strains can be produced in the crystal lattice of the individual crystallite. XRD method can measure the interatomic spacings, which are indicative of the elastic strain in the specimen. Changes in the interatomic spacing can, therefore, be related to the elastic strain in the material and hence, to the stress (James and Cohen, 1978).This technique uses repeated scanning of a selected peak with the specimen orientated at an increasing angle to the incident beam shown in Figure 2.6.

The x-ray beam is directed onto the sample surface at the location of interest. The diffracted beam is detected by a position-sensitive proportional counter. The angular position (2θ) of the diffracted beam is used to calculate the distance (d-spacing) between parallel planes of atoms using Bragg's law (satish, 2001) shown in equation 2.8. A series of measurements made at different x-ray beam approach angles (ψ) are used to fully characterize the d-spacing.

$$n\lambda = 2dsin\theta \qquad 2.8$$

Where

λ is the wavelength; *d* is the inter-planar spacing

θ is the angle between theIncident ray and the scattering planes

n is the order of reflection

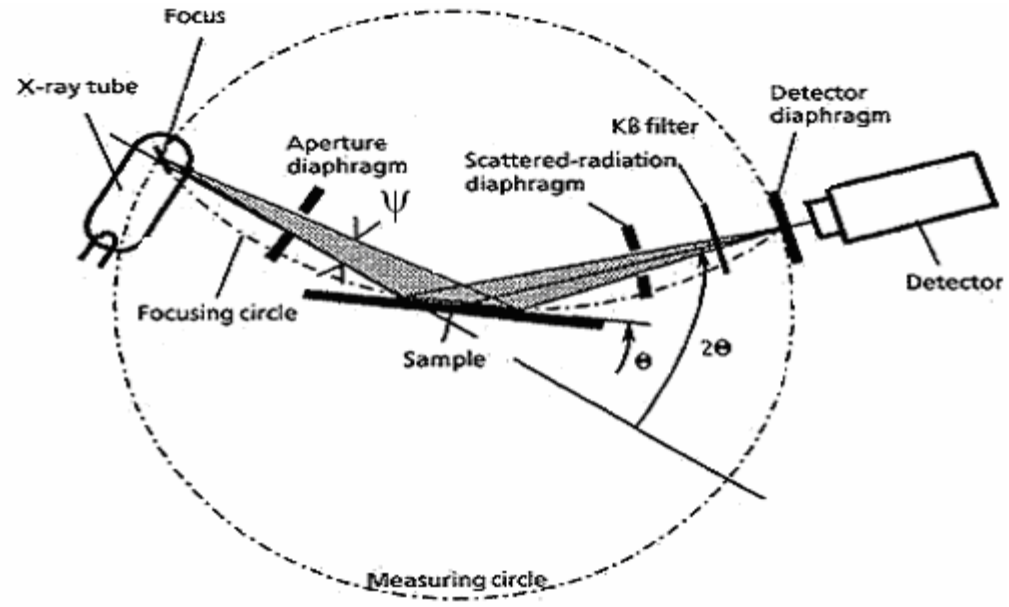

Figure 2.13: Conventional XRD Testing Principle (Satish, 2001)

The elastic strains (corresponding to the change of interplanar lattice spacing) can be readily calculated from equation 2.9 (Hilley,1971)

$$\varepsilon = \frac{d - d_0}{d_0} = \frac{\Delta d}{d_0} \quad 2.9$$

Here *d* is the deformed lattice spacing; $d_0$denotes the unstrained lattice spacing

Subsequently the stress is calculated from equation 2.10 (Hilley, 1971)

$$\sigma = \frac{d_\psi - d_0}{d_0}\left(\frac{E}{1 + \square}\right)\frac{1}{sin^2\psi} \quad 2.10$$

For measurements of strain a portable X-ray Diffractometer would be used. For the highest peak variation (Δθ) in the crystal lattice, the highest possible angle (θ) would be chosen to determine the diffraction peak. An excellent condition of analysis is the determination of the deformation of {420} planes in ferritic or martensitic steel.

The method that would be used is the two angle technique, with measurement of ψ = 0°, 20°, 30°, 40°, 50° and 60°.

In the two angle technique, the lattice spacing is considered as a linear function of $\sin^2\psi$.The technique has been thoroughlyinvestigated by the Society of Automotive Engineers(SAE) and finds wide acceptance in the United States. Selecting ψ angles to provide as large a range of$\sin^2\psi$ as possible within the limitations imposed by thediffraction angle 2θ and the sample geometry maximizessensitivity of the method. Lattice spacing is determinedprecisely at two extreme values of ψ, typically 0 and 45°,and the stress is calculated using equation 2.10.The specimen to be measured was mounted on joint X-ray/detector tube and rotated according to the specified ψ angles in the direction of the residual stress to be measured. XMAS software was used for generating the X-ray diffraction patterns, followed by computation of the longitudinal and transversal of the residual stresses(Cook et al, 2006).

Figure 2.14: X-ray Diffractometer XRD-6000 (National Steel Raw Materials Exploration Agency, Kaduna)

2.4.2.2 Neutron Diffraction Technique

The Neutron Diffraction (ND) method relies on elastic deformations within a polycrystalline material that cause changes in the spacing of the lattice planes from their stress-free value. Although stress measurements by XRD method are well established, they are practically limited to the near-surface stresses. Measurements by ND are carried out in much the same way as with XRD, with a detector moving around the sample, locating the positions of high intensity diffracted beams. A major advantage that neutrons have over x-rays is their capability to penetrate into greater depths that can make them suitable for measurement at depths ranging from around 0.2mm to about 1 cm. With high spatial resolution, ND can provide complete three-dimensional strain maps of many engineered components. This is achieved through translational and rotational movements of the component(International Atomic Energy Agency, 2003).

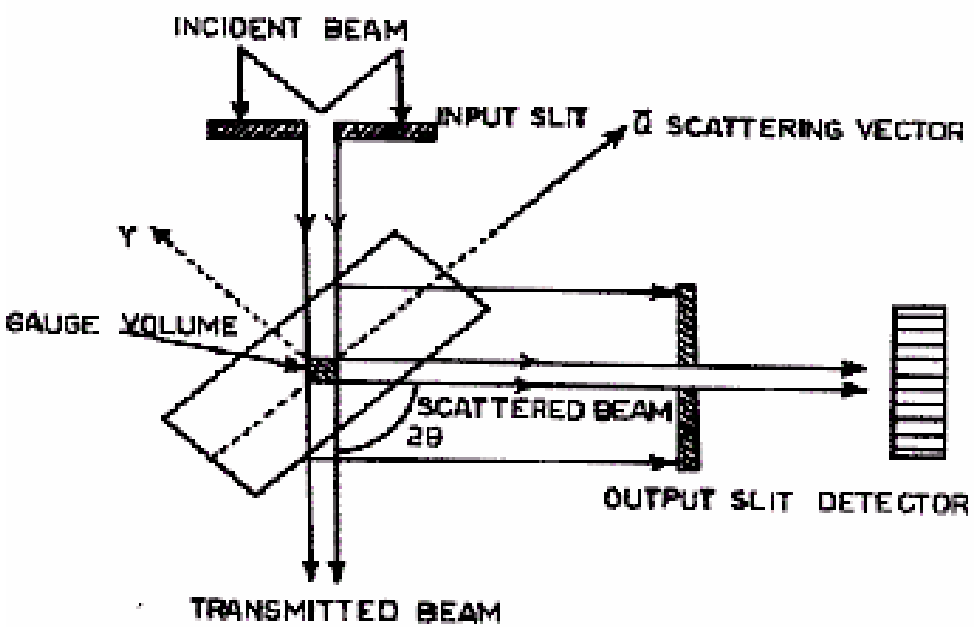

Figure 2.15: ND Experimental Principle(International Atomic Energy Agency, 2003)

2.4.2.3 Ring – Core Technique

The ring-core (RC) method is a mechanical/strain gage technique used to determine the principal residual stress as a function of depth in polycrystalline and/or amorphous materials. This method involves the localized removal of stressed material using an incremental ring coring or a mechanical dissection device, and measurement of strainrelief in the adjacent material. Strain gage rosettes (SGR) are usually used to measure the relieved strains(Keil, 1992).

Figure 2.16 : Experimental setup for Ring core method(Keil, 1992)

2.4.2.4 Sectioning Technique

Is a destructive method that relies on the measurement of deformation due to the release of residual stress upon removal of material from the specimen. It has been used extensively to analyze residual stresses in structural carbon steel, aluminum and stainless steel sections. The sectioning method consists in making a cut on an instrumented plate in order to release the residual stresses that were present on the cutting line. For this, the cutting process used should not introduce plasticity or heat, so that the original residual stress can be measured

without the influence of plasticity effects on the cutting planes' surface. The strains released during the cutting process are generally measured using electrical or mechanical strain gauges. In general, the strips of material released by the sectioning process may exhibit both axial deformation and curvature, corresponding to membrane and bending (through thickness) residual stresses, respectively. Membrane residual stresses σ_m generally dominate in hot rolled and fabricated sections whereas bending residual stresses σ_b are generally dominant in cold formed sections(Hasan, 2009).

2.4.2.5 Ultrasonic Method

One of the promising directions in the development of non destructive techniques for residual stresses measurement is the application of ultrasound. Ultrasonic method, called also refracted longitudinal wave techniques, is not limited by the types of material understudy and can be utilized for residual stresses measurements on thick samples. Ultrasonic stress measurement techniques are based on the acoustic-elasticity effect, according to which the velocity of elastic wave propagation in solids is dependent on the mechanical stress. The most important advantages of the development technique and equipment is the possibility to determine the residual and applied stresses in samples and real structure elements(Withers and Bhadeshia, 2001).

2.4.2.6 Hole – Drilling Method

This method is relatively simple and quick, it is one of the most popularly used semi destructive methods of residual stress evaluation which can provide the measurement of residual stress distribution across the thickness in magnitude, direction and sense. It has the advantages of good accuracy and reliability, standardized test procedures, and convenient practical implementation. The damage caused to the specimen is localized to the small, drilled hole, and is often tolerable or repairable. The principle involves introduction of a

small hole (of about 1.8 mm diameter and up to about 2.0 mm deep) at the location where residual stresses are to be measured. Due to drilling of the hole the locked up residual stresses are relieved and the corresponding strains on the surface are measured using suitable strain gauges bonded around the hole on the surface. From the strains measured around the hole, the residual stresses are calculated using appropriate calibration constants derived for the particular type of strain gauge rosette used as well as the most suitable analysis procedure for the type of stresses expected(Rossinia et al 2007).

Figure 2.17: Hole Drilling Rosette setup(http://www.residualstress.org)

For the purpose of this thesis, only the X-ray Diffraction Method would be considered.

2.5 Review of Related Works

Gurinder,(2013) carried out a research on finite element simulation of residual stress in butt welding of two AISI 304 stainless steel plates using a finite element based commercially available software, coupled thermal-mechanical three dimensional finite element model was developed by making an approximate geometry of the butt welded joint. Finite element analysis was performed to understand the complete nature of residual stresses in manual metal arc welded joint of AISI 304 stainless steel plate. Variation of residual stress in the plates in the heat affected zone was also studied. The results obtained by finite element method agreed with those from X-ray diffraction method as published in literature for the prediction of residual stresses.Welding operational parameters were: travel speed 2 mm/sec, arc voltage 22 Volts, arc current 65 Amps and efficiency 75% It was seen that the residual stress in the transverse direction for butt welding of 6 mm thick plates comes out to be maximum (288.97MPa) in the centre of weldment The lower value of welding current resulted in lower heat inputs and lower residual stresses.Residual stress increases with increase in plate thickness. Arc voltage and welding current have direct effect on the residual stress in the welding process as increase in the voltage and current increases heat input thus increasing residual stresses. Also, increase in welding speed reduces residual stresses but reduces quality of weld as well.

Jeyakumar *et al*, (2013) carried out a thermo-mechanical 3D finiteelement analysis to assess the residualstresses in the butt-weld joints of ASTM A36 steel plates utilizing the commercial software package ANSYS. The finite element model was employed to evaluate transient temperaturedistribution and the residual stress fields during welding.

Convective and radiative heat losses were taken into account throughboundary conditions for the outward flux. The residual stressdistribution and magnitude in all directions and equivalent stress were obtained. The weld geometry was (100 x 100 x 3) mm.

The peak temperature was recorded at 1973K. The analysis result of transverse residual stress varied from380.8 MPa (tensile) to -77.5 MPa (compressive). The residual stress (σ_x) distribution in the longitudinal varied from 387 MPa (tensile) to -1 MPa (compressive) while the longitudinal residual stress (σ_y) distribution varied from 108 MPa (tensile) to -497 MPa (compressive).

Harshal, (2012) Carried out a simulation of the complex arc welding process by using the finite element method with ANSYS Multiphysics. After the model was built and verified, the research studied the effects of varying the welding process parameters on the thermo-mechanical responses. In addition to that, the research also found a relationship between welding parameters and thermo-elastoplastic responses. The responses of single pass corner-joint of arc welding were evaluated through the finite element software (ANSYS Multiphysics).The study of this research paper covered only the effects of varying heat input, welding speed on the thermo mechanical responses of the weldment after cooling down to room temperature.

The heat input relationship was based on the following equation(Denga, 2007)

$$Q=V\times I\times 60/v \quad 2.11$$

Where, I is welding current; *V* is welding arc voltage; *v* is the arc welding speed, and Q is the heat input. In this work, the effect of heat input on welding responses wasevaluated using three values (heat input in Watt), characterized as low, medium, andhigh.As heat input increases stresses decreases, this is due to the fact material propertiessuch as young's modulus decreases as temperature in the material increases. As the heatinput increases temperature generates in the plate increases and thus the stressgenerated

decreases.Welding speed represents the distance of the torch travelled along the weld line per unitof time. The heat input is inversely proportional to the welding speed. Therefore, whenthe heat input is larger; the welding speed is slower for a constant heat input rate.In this research, low, medium, and high welding speeds were investigated while considering the rest of parameters such as heat input is kept at low value and restraintsat high value.As the speed of welding increases the stresses induced in the plate decreases because as welding speed increase time for welding decreases and thus it is noted that the fasterthe welding speed is made, the less heat is absorbed by the base metal and thus stressesinduced decreases.

Stamenkovic *et al,* (2009) performed a 3D residual stress analysis of butt-weld joint of ASTM 36 steel plates (100 x 100 x 3mm) with arc efficiency, n =0.85, arc voltage (V)= 24 V, the current (I)= 180A, r_b= 3 mm and welding speed = 5 mm/sec. The peak temperature reached 1973K. And tensile stresses were developed in the weld zone.These tensile stresses gradually decreased in the transverse direction awayfrom the weld center line and became compressive towards the edge of the plate. The residual stress (σ_x) transverse varies from 383 MPa (tensile) to -78 MPa (compressive). The residual stress (σ_y) varied from 80 MPa (tensile) to -543 MPa (compressive). The residual stress (σ_x) distributionthrough thickness at weld center line (longitudinal) varied from 388 MPa to 384MPa (tensile) also the residual longitudinal stress (σ_y)through thickness at weld center line varied from 72.5 MPa to 50.8MPa (tensile).

CHAPTER 3

MATERIALS, EQUIPMENT AND METHODS

3.0 Introduction

This chapter describes details of materials, equipments and experimental procedure used to carry out the welding experiment and the process simulation for determining the theoretical and experimental residual stresses.

3.1 MATERIALS

The materials used in this workfor the specimen welding are listed below:

i. Low carbon steel (ASTM A36) plates
ii. E6011 Electrode filler metal

3.2 EQUIPTMENT

The equipments used in this research both for the experiment and the finite element simulation are listed below:

i. Shielded metal arc welding machine
ii. X-ray diffractometer (XRD 6000)
iii. Wire brush
iv. Clamps
v. ANSYS Multiphysics V14
vi. Computer system

vii. Nitric Acid

viii. XMAS 2.0 Software

3.2.1 Shielded manual arc welding machine

The specifications and operating parameters of the shielded manual arc welding machine used in this research are shown in Table 3.1 below:

Table 3.1: Specifications and Operating Parameters of Shielded manual arc welding machine

Parameter	**Specification**	**Value**
Arc efficiency	η	0.75
Voltage	V	25V
Current	I	90A
Welding Speed	υ	2mm/sec
Electrode diameter	x	3.142mm
Base metal	Thickness	6mm
Filler metal	Electrode	E6011
Welding position	Orientation	Flat
Bevel groove	Angle	60°
Root opening	Depth	2mm

3.2.2 X-ray Diffractometer

The model of the X-ray diffractometer used is the XRD-6000. The specifications and operating parameters as used in this research are tabulated below

Table 3.2:X-Ray Diffractometer Operating Parameters

Parameter	**Specification**
Material	Low carbon steel
Bravers lattice	BCC[5]
X-ray tube anode	CrK- α
K-β filter	V
2-Theta angle	156.1
{hkl}	{211}
Multiplicity	24
Target	Cr
Voltage (V)	40.0 KV
Current (I)	30.0 mA
Ψ range	(0,20,30,40,50,60)°
Wavelength (λ)	2.2897Å (Cr-K) α

3.2.3 Computer system

The specifications of the computer work station used to carry out the finite element model simulation are shown in the Table 3.3:

Table 3.3: Computer System Specifications

Specification	Description
Operation	Windows 8 pro
Processor	Intel(R)Core(Tm)i7-3612QM,CPU @2.10GHz
Installed memory (RAM)	12.0 GB
System type	64-bit OS, x64-based processor

Hard disk	1 terabyte

3.3METHODS

3.3.1 The Welding Process

The welding of the specimen was carried according to ASTM international welding standard procedure and is outlined below.

i. Preparation of the weld joint

   a) The surface of the weld joint was then cleaned of rust, scales, dirt, oil and grease using nitric acid.

   b) The edges of both plates to be joined were machined to have a bevelled V-groove angle of 60°.

   c) The root depth of 2mm between both plates was allowed to ensure full penetration of the weld.

ii. Fixturing and positioning

   a) The weld specimen were then placed on a rig and clamped to ensure minimizing distortion caused during welding.

   b) The specimen were aligned properly (fit up) to ensure proper quality weld and increased efficiency.

iii. Application of heat input

   a) The weld was executed in the flat position in a single pass which lasted 50 seconds.

b) The heat input was quantified based on equation 2.7.

iv. Post weld practice

a) The weld was allowed to cool down to room temperature.

b) All slag inclusions were removed from the heat affected zone using a wire brushand the joint washed in a solution of nitric acid.

c) The welded joint was inspected for uniformity.

d) Three welded samples were produced.

3.3.2 Welding Precautions

These welding precautions were adhered to during the experimental welding process to ensure that the samples were produced according to specification (American Welding Society, 2001).

i. The specimen was firmly held in place by the clamps to the work table to ensure the reduction of distortion. Due to the application of the filler metal, the steel plates are likely to misalign and produce distorted samples. As a result, the steel plates have to be rigidly clamped on the work bench.

ii. The ASTM A36 steel plates were cleaned to remove any dirt and oil deposits present on the welded surfaces to ensure little contamination of the weld. These impurities if left unchecked would affect the integrity of the weld.

iii. All welding parameters specified in the thesis were adhered to during the welding process. That is the current, voltage, and weld speed.

iv. All protective gear was used to prevent the occurrence of any accidents (rubber gloves, overall covers, protective glasses.

v. The process was efficiently timed to ensure the movement of the electrode was maintained at about 2mm/s and the weld was completed in 50 seconds.

vi. The welding was carried in a well ventilated area to prevent weld fume poisoning. (http://www.navybmr.com/studymaterial/14250a/14250A_ch8.pdf, accessed on 10th Octeber,2015)

3.3.3 X-Ray Diffraction Measurement process of Residual Stress

The x-ray diffraction measurementof residual stress was carried according to standard procedure as outlined in Shimadzu xrd-6000 operation manual . The procedure is highlighted below:

i. Specimen preparation
    a) All soil, grease, dirt and slag on the welded surface were removed by cleaning the specimen.

ii. Positioning of Specimen
    a) The specimen to be measured was mounted on the sample surface in the horizontal direction.
    b) The region spanning across the surface of the weld was chosen for residual stress measurement. Thus ensuring that the surface coincided with the center of rotation of the goniometer.

iii. Measurement of residual stress
    a) The X-ray of monochromatic wavelength was generated and incident on the specimen.
    b) The diffracted beams were received at the detector and the diffraction patterns collected.

c) The specimen was tilted in the direction of the desired residual stress to the measured.

d) Five tilt angles were used for both negative and positive Ψ.

e) The diffraction peaks were obtained and the desired strain and residual stress was calculated using XMAS 2.0 software.

3.3.4 Precautions in X-Ray Diffraction Measurement of Residual Stress

i. The sample was properly cleaned of all dirt, oil and fluids before being mounted on the X-Ray machine. The presence of contaminates would affect the angle of the diffracted x-ray after it incidents on the surface of the sample. This would cause in error in determination of the strains in the lattice spacing (Jamesand Cohen,1978).

ii. Because the diffraction angles must be determined to accuracies of approximately ±0.01°, the sample was positioned in the x-ray beam at the true center of rotation of the ψ and 2θ axes, and the angle ψ was kept constant throughout the irradiated area. Thus, extremely precise positioning of the sample to accuracies of approximately 0.025 mm (0.001 in.) is critical(Fitzpatrick et al, 2005).

iii. The size of the irradiated area was limited to an essentially flat region on the sample surface. Small diameter samples or such sample geometries as small-radius fillets, the roots of threads, and fine-pitched gears may contribute to major sources of error if the x-ray beam is not confined to an essentially flat region at a known tilt ψ on the curved surface. (Cook *et al*,2006).

iv. The X-Ray Diffractometer was run at the designated operating parameters to ensure emission of the desired x-rays and proper diffraction after incidence on the sample.

3.4 Finite Element Model

In this study, the butt-weld joint of two mild steel plates was modelled using ANSYS Multiphysics V14. To simplify the welding simulation, the thermal and mechanical analysis was performed separately.

3.4.1 Thermal Analysis.

Thermal analysis helps understand how the material would behave under temperature dynamics. Transient thermal analysis was used as it determines the temperature values from the transient analysis as a result of the heat flux input.

i. DefiningElement type
    a) The element type SOLID70 was used for the thermal analysis. This element type is auto assigned for thermal analysis by the ANSYS Multiphysics software V14 but manually assigned in ANSYS Mechanical or lower versions of the software.
    b) GUI method: ANSYS main menu > pre-processor > element type > SOLID70

ii. Defining material properties
    a) The properties needed are thermal conductivity, specific heat and density.
    b) The material properties were assigned on the materials property interface in ANSYS Multiphysics as shown in figure

iii. Geometrical Modelling
    a) The geometry of the model in which the residual stress is to be simulated was created in ANSYS Multiphysics design modeller.

b) Three volumes were created for the model. The first and third volume are the (metal plates) and the second was the filler metal. The dimension of the model is as per Figure 3.1.

iv. Meshing

a) Meshing is a method in which the model is sub divided into small pieces of simple shapes (elements) connected at common points (nodes).

b) The automatic mesher in the software was used to generate a mesh based on a global element size, tolerance, and local mesh control specifications.

v. Defining analysis type.

a) Transient thermal analysis was used to determine the temperature values from the transient analysis as a result of the heat flux input.

b) GUI method: ANSYS main menu > Solution > Analysis Type > New Analysis > Transient > Full

vi. Setting the Solution Control

a) The time at the end of the load step was set to 1s.

b) Automatic time stepping was turned off.

c) The number of load steps was set to 1, thus the solution was done every 1 second at the end of each load step.

d) The total number of load steps was set to 50.

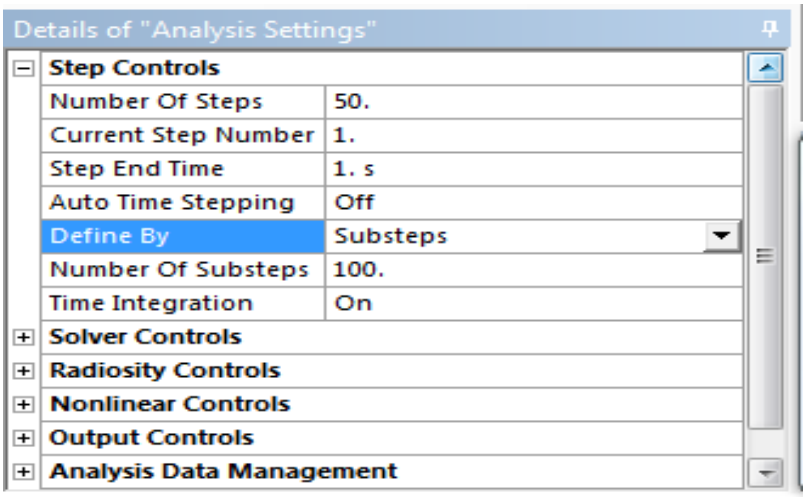

Figure 3.1: Setting the solution control

vii. Applying boundary Conditions

a) The bulk air temperature was set to be 27^{o}C.

b) Convection heat transfer was applied on the model based on equation 2.6.

viii. Defining the Heat load input to the model

a) Heat input during welding simulation was modelled by a distributed heat flux applied on the individual elements.

b) The heat was applied through birth and death technique. The birth and death technique was used to deactivate and reactivate selected elements thus simulating filler material deposition in the welding process.

c) Heat input is that which is obtained from the experimental process.

d) GUI method: ANSYS main menu > Solution > Define Loads > Apply > Thermal > Heat Flux

ix. Solution and Result

a) The solve command was initiated after all the temperature profile, boundary conditions and parameters for the thermal analysis were inputted.

b) The result obtained from the transient thermal analysis was applied to the structural analysis as a load step to enable determination of the residual stresses.

3.4.2 Structural Analysis

The structural analysis was conducted to determine the effects of thermal loads on the physical structure of the metal.Structural properties of the metal such as yield strength, tensile strength, poison ratio, young modulus and melting point are required for the complete structural analysis. The geometry and meshing are the same as used in the thermal analysis.

i. Change element type

GUI method: ANSYS main menu > pre-processor > element type > switch Elem Type.

The element type SOLID70 which was used for the transient thermal analysis would be replaced with SOLID 185.

ii. Definition ofMaterial Properties

a) The structural properties were defined according to table to perform the structural analysis.

b) GUI method: ANSYS main menu > pre-processor > material props > materials models.

iii. Specifying initial Conditions

a) Both ends of the plates were clamped by assigning the displacement to zero at both ends of the plates.

b) GUI method: ANSYS main menu > pre-processor > loads > Apply > structural Displacement > On Nodes.

c) The reference temperature was assigned.

d) GUI method: ANSYS main menu > solution > Define loads > settings > Reference Temp.

iv. Solve

a) The temperature from the thermal analysis was applied as a thermal load in the structural analysis.

b) GUI method: ANSYS main menu > Solution > Define Loads > Apply > Structural > Temperature > From Thermal Analysis.

c) The solve command was initiated after all the temperature profile, boundary conditions and parameters for the structural analysis were imputed.

All values of residual stress were obtained and the stress intensity plots generated.

3.5 Statistical analysis of results

Statistical analysis of the experimental values of residual stress obtained from the X-ray diffraction and the simulated values from the finite element analysis was carried out.

i. A correlation coefficient test was carried out to determine their level of correlation.

ii. F-Test was performed to show that the level variance of residual stress values are not significant

CHAPTER 4

RESULTS AND DISCUSSION

4.0 Introduction

The result from the residual stresses obtained from the X-ray diffraction experiment and finite element model simulation are presented and discussed in this chapter.

4.1 Results

The results from the x-ray diffraction and the Finite Element Model (thermal and structural analysis) were evaluated to obtain the values of the residual stresses developed during the welding process. These results are as follows;

4.1.1 Temperature Distribution

The contour plot in Figure 4.1 shows the temperature distribution on the plate at 25 seconds of the Finite Element Model Simulation.

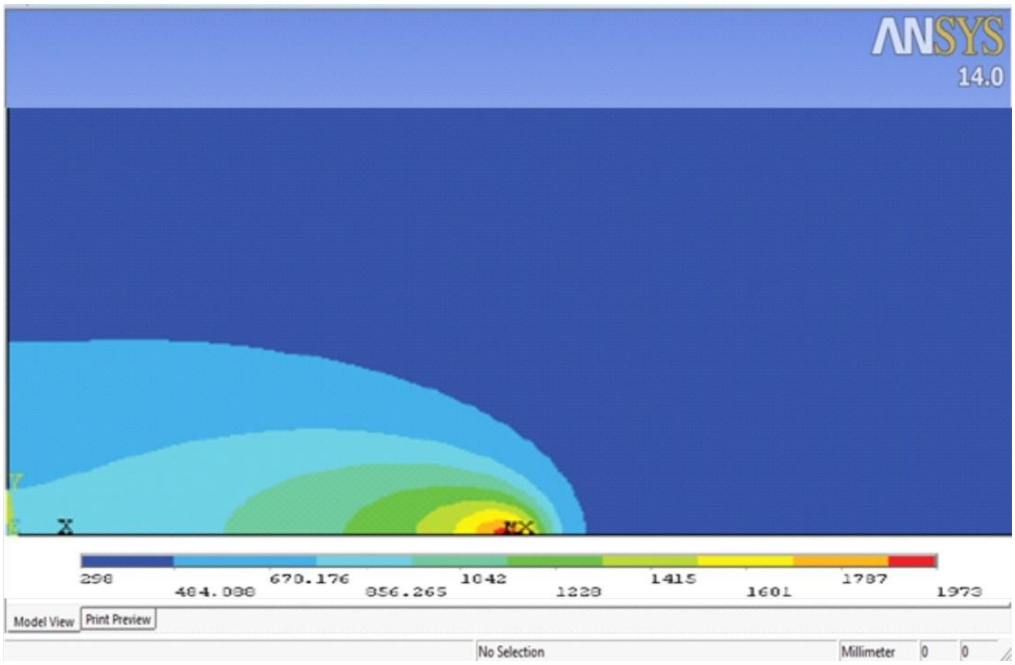

Figure 4.1 Contour Plot Temperature distribution on the plate at 25 seconds

Figure 4.2 shows the temperature variation with distance along the transverse direction on the steel plates away from the Heat affected zone.

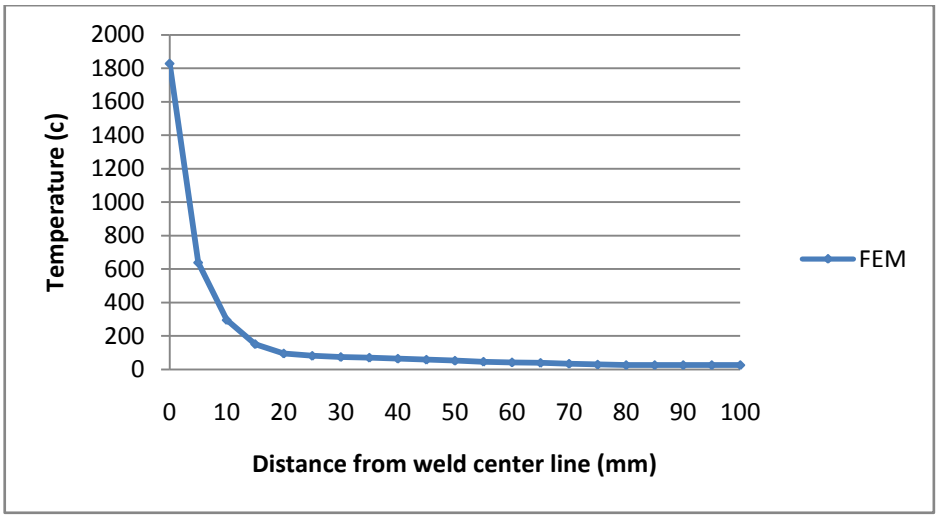

Figure 4.2 Temperature variation with distance along the transverse direction

4.1.2 Stress Intensity Plot

The stress intensity plot generated after the completion of the simulation is shown in Figure 4.3.

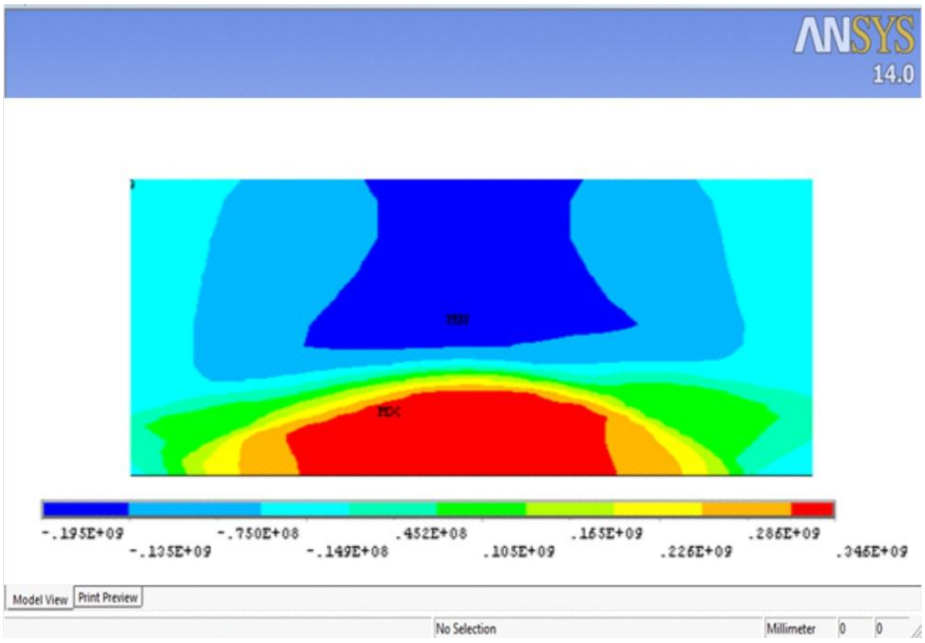

Figure 4.3 Contour plot of residual Stresses (N/m^2)

4.1.3 Experimental samples of Butt Welded ASTM A36 low Carbon Steel produced

The heat input was quantified based on equation 2.7

$$Q = \frac{0.75\ x\ 25\ x\ 90}{2\ x\ 3.142} = 268.539147(\frac{W}{mm^2})$$

Three samples of ASTM A36 low carbon steel plates of dimension 200mm x 100mm x 6mm from which the residual stresses generated during the welding process were measured and produced as shown in Figure 4.4

Figure 4.4 Experimental samples of Butt Welded ASTM A36 low Carbon Steel

4.1.4 Residual Stress Values Obtained

The residual stress generated from the Shielded manual metal arc welding of the steel plates measured by the X-ray Diffractometer and the expected values as simulated by the finite element model as presented as follows;

4.1.4.1 Experimental Residual Stress values obtained

The Transverse residual stresses (σ_x) of the three samples measured by the X-ray diffractometer are shown in Table 4.1

Table 4.1: Transverse residual stresses (σ_x) of the three samples

	Transverse residual stresses σ_x (MPa)

Point (cm)	Sample 1	Sample 2	Sample 3	Mean ($\overline{\sigma}_x$)
0	354.9	354.8	351.4	353.7
10	277.2	273.5	275.5	275.4
20	-126.8	-127.7	-127.1	-127.2
30	-202.0	-200.9	-199.8	-200.9
40	-95.6	-99.1	-97.2	-97.3
50	-21.8	-23.6	-25.1	-23.5
60	-5.8	-4.7	-4.8	-5.1
70	-3.7	-3.9	-3.8	-3.8
80	-1.1	-1.1	-1.4	-1.2
90	1.9	1.6	2.2	1.9
100	3.1	3.3	2.9	3.1

The Transverse residual stresses (σ_y) of the three samples measured by the X-ray diffractometer are shown in Table 4.2

Table 4.2: Transverse residual stresses (σ_y) of the three samples

Point (cm)	Transverse residual stresses σ_y (MPa)			
	Sample 1	**Sample 2**	**Sample 3**	**Mean ($\bar{\sigma}_x$)**
0	165.2	165.5	164.6	165.1
10	175.3	174.1	170.8	173.4
20	146.8	148.1	146.7	147.2
30	95.9	95.3	96.8	96.0
40	68.7	69.9	69.0	69.2
50	44.8	46.2	44.9	45.3
60	26.0	26.1	25.0	25.7
70	19.2	21.3	19.8	20.1
80	16.0	15.8	16.2	16.0
90	5.0	5.1	5.5	5.2
100	0	0	0	0

The Longitudinal residual stresses (σ_x) of the three samples measured by the X-ray diffractometer are shown in Table 4.3

Table 4.3: Longitudinal residual stresses (σ_x) of the three samples

Point (cm)	Longitudinal residual stresses σ_x (MPa)			
	Sample 1	**Sample 2**	**Sample 3**	**Mean ($\overline{\sigma}_x$)**
0	0	0	0	0
10	166.8	163.5	161.1	163.8
20	285.9	286.3	284.0	285.4
30	314.6	316.2	318.1	316.3
40	326.3	325.7	325.1	325.7
50	336.2	336.9	329.2	334.1
60	331.9	332.1	333.8	332.6
70	324.4	327.2	329.4	327.0
80	299.1	295.4	298.0	297.5
90	49.9	51.6	49.4	50.3
100	3.9	3.1	3.8	3.6

The Longitudinal residual stresses (σ_y) of the three samples measured by the X-ray diffractometer are shown in Table 4.4

Table 4.4: Longitudinal residual stresses (σ_y) of the three samples

Point (cm)	Longitudinal residual stresses (σ_y)			
	Sample 1	**Sample 2**	**Sample 3**	**Mean ($\overline{\sigma}_x$)**
0	-319.4	-322.8	-318.4	-320.2
10	-245.6	-242.1	-242.8	-243.5
20	55.7	56.9	57.8	56.8
30	144.3	140.1	140.7	141.7
40	169.2	172.0	172.1	171.1
50	161.6	153.4	163.2	159.4
60	136.4	133.7	136.7	135.6
70	118.2	124.1	121.6	121.3
80	-31.8	-34.0	-33.5	-33.1
90	-234.8	-235.7	-235.1	-235.2
100	-275.0	-274.2	-270.7	-273.3

4.1.4.2 Residual Stresses Generated from Finite Element Simulation

The residual stresses generated from the Finite Element model of the steel metal plates is shown in Table 4.5

Table 4.5: Residual stresses generated from the Finite Element model

	Transverse Residual Stresses (MPa)	**Longitudinal Residual Stresses (MPa)**

Point (cm)	σ_x	σ_y	σ_x	σ_y
0	365.4	153.4	0	-350.2
5	375.2	172.8	75.3	-375.6
10	310.8	168.3	185.1	-200.4
15	115.6	165.1	277.7	-69.8
20	-115.1	141.7	300.2	81.0
25	-183.7	117.3	318.6	124.2
30	-167.3	82.6	327.9	165.3
35	-116.2	66.9	342.4	167.8
40	-78.5	59.2	351.0	160.1
45	-43.4	49.1	352.1	152.6
50	-15.3	38.5	353.2	135.2
55	0	29.2	354.1	129.0
60	4.2	17.0	355.7	123.4
65	8.1	12.9	352.3	116.7
70	12.9	9.2	349.6	101.3
75	15.7	8.3	341.4	84.2
80	17.3	5.1	335.9	72.9
85	19.0	0	283.2	-200.5
90	21.6	0	138.8	-185.9
95	25.4	0	-10.2	-285.3
100	28.2	0	-10.1	-300.1

4.1.5 Comparison of Residual Stresses from X-Ray diffraction and Finite Element Model Simulation

Figure 4.5 shows the graphical presentation of the residual stress result obtained from the x-ray diffraction and FEM simulation of the transverse residual stress (σ_x) along the weld line in the transverse direction.

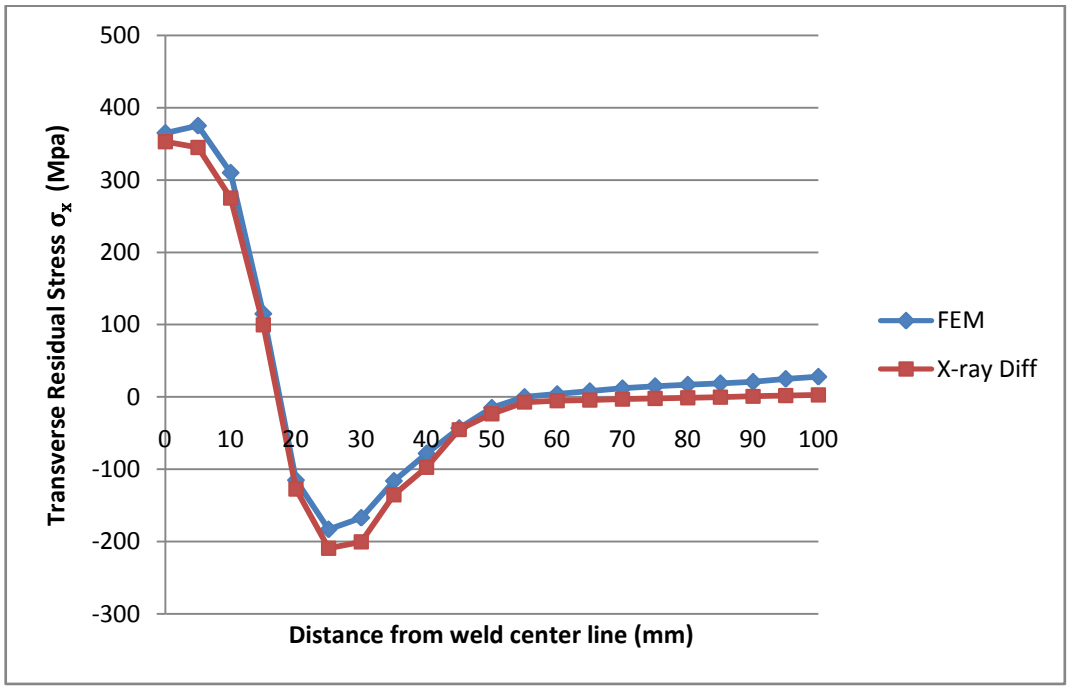

Figure 4.5 Comparison of the x-ray diffraction and FEM simulation of the transverse residual stress (σ_x) along the weld line.

Figure 4.6 shows the line graph comparison of the experimental and FEM transverse residual stress (σ_y) along the weld line in the transverse direction.

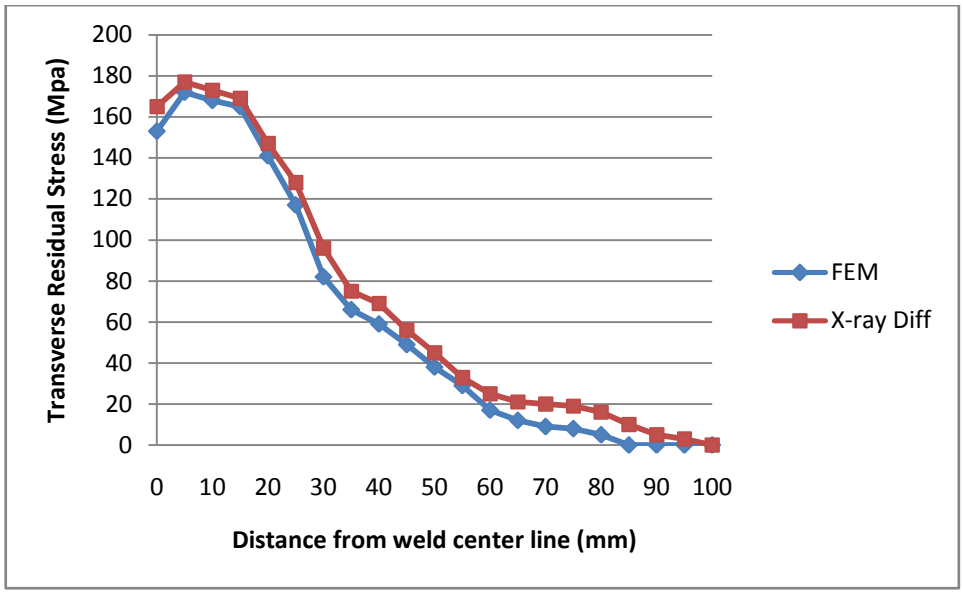

Figure 4.6 Comparison of the experimental and FEM transverse residual stress (σ_y) along the weld line

Figure 4.7 shows the x-ray diffraction and FEM simulation result of the longitudinal residual stress (σ_x) along the weld line in the longitudinal direction.

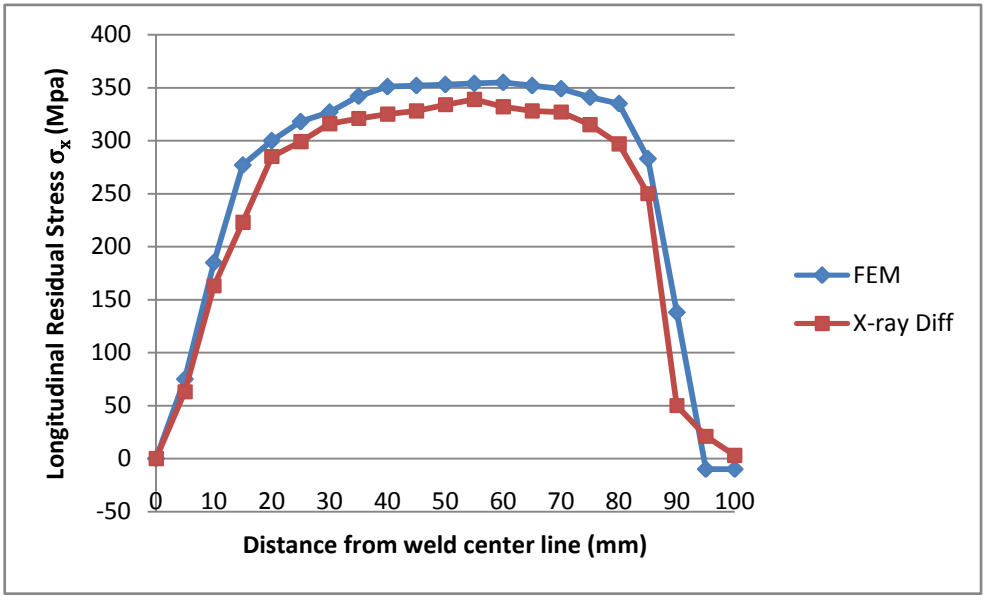

Figure 4.7 comparison of the x-ray diffraction and FEM simulation of the longitudinal residual stress (σ_x) along the weld line in the longitudinal direction

Figure 4.8 shows the line graph comparison of the experimental X-Ray Diffraction and FEM longitudinal residual stress (σ_y) along the weld line in the longitudinal direction.

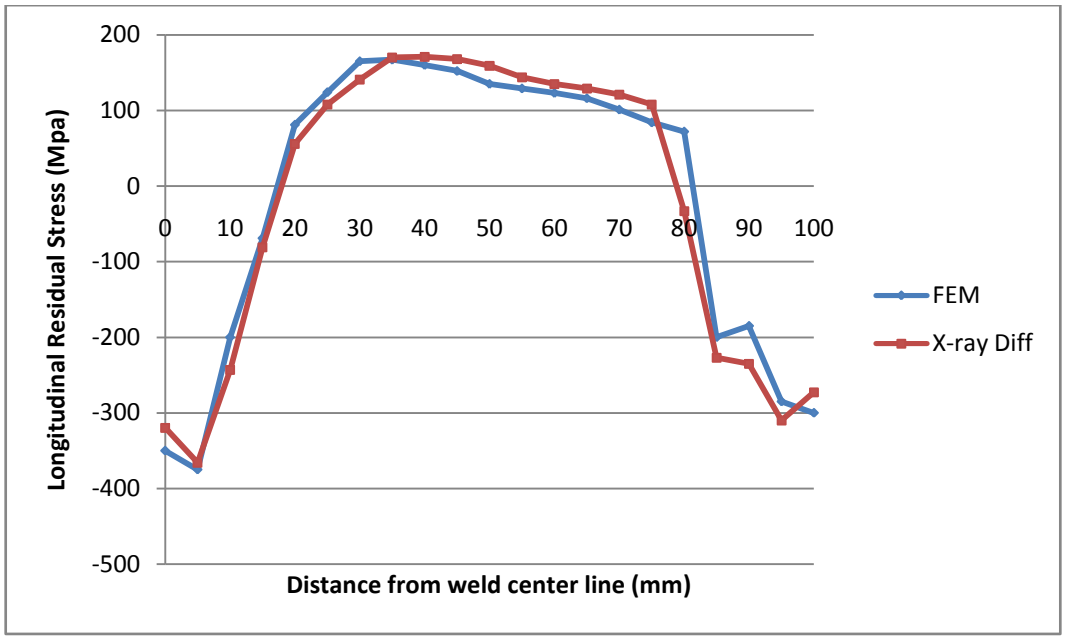

Figure4.8 Comparison of the experimental and FEM longitudinal residual stress (σ_y) along the weld line

4.1.6 Statistical Analysis of result

The residual stresses obtained from the X-Ray diffraction experiment and the finite element model were statistically analysed to determine their level of correlation. Acorrelation coefficient test and F-Test were carried out. Their results are presented in the Table 4.6.

Table 4.6 Correlation Coefficient and F-Test of Residual Stress

Residual Stresses	Correlation Coeff. Test	FTest

Transverse stress (σ_x)	0.99842767	0.968222988
Transverse Stress (σ_y)	0.998486295	0.998051236
Longitudinal stress (σ_x)	0.985773807	0.805315383
Longitudinal Stress (σ_y)	0.986306706	0.912312532

4.2 Discussion of the Results

The results obtained from the experiment and Finite Element Simulation are discussed as follows.

4.2.1 Temperature Distribution

Referring to the contour plot in Figure 4.1, the temperature distribution on the plate and the Maximum temperature can be seen from the contour plot. Heat flux was 268e6 (W/m^2). The initial temperature was 27°C and convection coefficient of 15W/m^2C. The maximum temperature shown was at 1827°C at the node as the heat flux moved along the weld line. Which in real case was the arc produced by the electrode.

Figure 4.2 shows the temperature variation with distance along the transverse direction on the steel plates away from the HAZ. It can be seen that the temperature is maximum around the line of the welding and gradually reduces towards the edge of the plate.The maximum temperature was 1827°C while that at the end of the plate was maintained at around 27°C. This is similar to the result obtained by (Stamenkovic and Ivana, 2009).

4.2.2 Stress Intensity Plot

The stress intensity plot shown in Figure 4.3 indicates the accumulation of stresses around the filler metal which is the HAZ region. Based on the intensity plot, the transverse stress in the x direction (σ_x) had a maximum value of 375Mpa (tensile) and minimum value of -183Mpa (compressive) while in the y direction (σ_y), the maximum value of 172Mpa (tensile) and minimum value of 0.

The longitudinal stress in the x direction (σ_x) indicated a maximum value of 355Mpa (tensile) and a minimum value of -10 (compressive) while in the y direction (σ_y), the maximum value was 167Mpa and the minimum value of the residual stress was -375Mpa. This is in agreement with the result obtained by (Jeyakumar *et al*, 2013).

4.2.3Experimental samples of Butt Welded ASTM A36 low Carbon Steel produced

Figure 4.4 shows the three samples of ASTM A36 low carbon steel plates of dimension 200mm x 100mm x 6mmproduced from the shielded manual metal arc welding process. This is similar to the geometry used by (Jeyakumar et al, 2013). The basic variation is the length of the steel plate which is 100mm, while in this work 200mm length was used. This would have very little influence on the expected residual stress since the weld zone is still at a satisfactory distance from the end of the plates.

4.2.4 Residual Stress values Obtained

4.2.4.1 X-Ray Diffraction Experiment values of Residual Stress measured

Table 4.1 shows the values of Transverse Residual (σ_x)stressesexperimentally measured by the X-Ray diffractometer. At the weld zone a residual stress of 353Mpa (tensile) was measured. This reduces and turned compressive along the steel plates away from the heat affected zone. A minimum value of about -200 MPa was recorded at a distance 30cm from

the weld center line. The value of residual stress was later noted to increase gradually as the end of the weld plate was reached.

Transverse Residual (σ_y)stressesexperimentally measured by the X-Ray diffractometer at the weld zone was 165Mpa (tensile). This reduced and turned compressive along the steel plates away from the heat affected zone and a minimum value of 0MPa was recorded at the end of the steel plate as shown in Table 4.2

Table 4.3 shows the values of Longitudinal Residual (σ_x)stresses experimentally measured by the X-Ray diffractometer. At the weld zone a residual stress of 0Mpa was measured. The residual stresses were tensile and increased along the steel plates away from the weld zone. A maximum value of 332MPa was recorded at 60cm from the HAZ. This reduced and turned compressive till the end of the weld plates.

Longitudinal Residual (σ_y) stresses experimentally measured by the X-Ray diffractometer at the weld zone was -320Mpa. This value increased and turned tensile along the steel plates away from the heat affected zone and a maximum value of 171MPa was recorded at a distance 40cm from the HAZ of the steel plate. From that point to the end of the steel plate, the residual stress reduced and turned compressive up to the end of the steel plates as shown in Table 4.4

4.2.4.2 Finite Element Simulation values of Residual Stress generated

Table 4.5 shows the values of Transverse Residual and Longitudinal Residualstresses generated from the 3D Finite Element modelling of the welding process with ANSYS Multiphysics V14.The transverse residual stress (σ_x) varied from 365Mpa (tensile) to -183Mpa (compressive). While the Transverse residual stress (σ_y) varied from 172Mpa (tensile) to 0. The Longitudinal residual stress (σ_x) varied from 355Mpa (tensile) to -10Mpa (compressive). While the Longitudinal residual stress (σ_y) varied from 167Mpa

(tensile) to -375Mpa (compressive). The Values of X-Ray Diffraction measured residual stresses agree with those from the Finite Element Simulation. This is also similar to the result obtained by Jeyakumar *et al*, (2013).

4.2.5 Comparison of Residual Stresses from X-Ray diffraction and Finite Element Model Simulation

With reference to Figure 4.5the line graph comparison of the X-Ray Diffraction and FEM simulation of the transverse residual stress (σ_x) along the weld line in the transverse direction is shown. The experimental XRD values varied from 353Mpa (tensile) to-209Mpa (compressive) while the FEM transverse residual stress varied from 365Mpa (tensile) to -183Mpa (compressive).

Figure 4.6 shows the comparison of the experimental and FEM transverse residual stress (σ_y) along the weld line in the transverse direction. The experimental value varied from 177Mpa (tensile) to 0 while the FEM value varied from 172Mpa (tensile) to 0.

Figures 4.5 and 4.6 shows that tensile stresses were developed in the weld zone. These tensile stresses gradually decrease in the transverse direction away from the weld center line and become compressive towards the edge of the plate. The peak tensile residual stress estimates from the X-ray diffraction measurement is in agreement with those obtained from the Finite Element Simulation Result. This is also in agreement (Stamenkovic and Ivana, 2009).

Figure 4.7 shows the comparison of the x-ray diffraction and FEM simulation of the longitudinal residual stress (σ_x) along the weld line in the longitudinal direction. The experimental values varied from 339Mpa (tensile) to 0Mpa (compressive) while the FEM longitudinal residual stress varied from 355Mpa (tensile) to -10Mpa (compressive).

Figure 4.8 shows the comparison of the experimental and FEM longitudinal residual stress (σ_y) along the weld line in the longitudinal direction. The experimental value varied from 171Mpa (tensile) to -366Mpa (compressive) while the FEM value varied from 167Mpa (tensile) to -375Mpa (compressive).

Figures 4.7 and 4.8 shows that tensile stresses were developed in the weld zone. These tensile stresses gradually decrease in the longitudinal direction away from the weld centre line and become compressive towards the edge of the plate. The peak tensile residual stress estimates from the X-ray diffraction measurement is also in good agreement with those obtained from the Finite Element Simulation Result. This is also similar to the result obtained by(Dean and Hidekazu, 2008).

4.2.6 Statistical Analysis of result

Statistical analysis was performed on the collected data. A Correlation coefficient was used to determine the level of correlation and F-Test to determine the significance of the level of variation.

4.2.6.1 Correlation Coefficient

The correlation coefficient between the Transverse Residual stresses (σ_x) of the X-Ray diffraction and Finite Element Simulation was 0.99842767 as shown in Table 4.6. This indicates a strong uphill (positive) linear relationship. Such that as the transverse residual stress of the experiment increases, that of the Finite Element Simulation also increases. And as the transverse residual stress of the experiment decreases, that of the Finite Element Simulation also decreases.

The correlation coefficient between the Transverse Residual stresses (σ_y) of the X-Ray diffraction and Finite Element Simulation was 0.998486295 as seen in Table 4.6. This

indicates a strong uphill (positive) linear relationship. Such that as the transverse residual stress of the experiment increases, that of the Finite Element Simulation also increases. And as the transverse residual stress of the experiment decreases, that of the Finite Element Simulation also decreases.

The correlation coefficient between the Longitudinal Residual stresses (σ_x) of the X-Ray diffraction and Finite Element Simulation was 0985773807 as shown in Table 4.6. This indicates a strong uphill (positive) linear relationship. Such that as the transverse residual stress of the experiment increases, that of the Finite Element Simulation also increases. And as the transverse residual stress of the experiment decreases, that of the Finite Element Simulation also decreases.

The correlation coefficient between the Longitudinal Residual stresses (σ_y) of the X-Ray diffraction and Finite Element Simulation was 0986306706 as indicated in Table 4.6. This indicates a strong uphill (positive) linear relationship. Such that as the transverse residual stress of the experiment increases, that of the Finite Element Simulation also increases. And as the transverse residual stress of the experiment decreases, that of the Finite Element Simulation also decreases.

4.2.6.2 F-Test

An F-Test was performed to show that the variances in the values of residual stresses for both the X-Ray diffraction and the Finite Element Model arenot significantly different.

The F-Test result for Transverse Residual stresses (σ_x) of the X-Ray diffraction and Finite Element Simulation was 0.968222988 as shown in Table 4.6. This value is close to unity(1) which indicates that the level of variation between both sets of data is not significant.

Also the F-Test result for Transverse Residual stresses (σ_y) of the X-Ray diffraction and Finite Element Simulation was 0.998051236 as shown in Table 4.6. This value is close to unity (1) which indicates that the level of variation between both sets of data is not significant.

The F-Test result for Longitudinal Residual stresses (σ_x) of the X-Ray diffraction and Finite Element Simulation was 0.805315383 as shown in Table 4.6. This value is close to unity (1) which indicates that the level of variation between both sets of data is not significant.

Also the F-Test result for Longitudinal Residual stresses (σ_y) of the X-Ray diffraction and Finite Element Simulation was 0.912312532 as shown in Table 4.6. This value is close to unity (1) which indicates that the level of variation between both sets of data is not significant.

CHAPTER 5

CONCLUSION AND RECOMMENDATION

5.0 Introduction

The conclusions and recommendations of this research are presented below.

5.1 Conclusion

i. A Finite Element Model for predicting residual stresses in ShieldedMetal Arc Welding of ASTM A36 low Carbon Steel Plates was successfully developed.

ii. The Shielded manual metal arc welding process was satisfactorily simulated using the finite element method in ANSYS Multiphysics Version 14 software.

iii. Three experimental samples of butt welded ASTM A36 mild steel plates were efficiently produced .

iv. The residual stresses developed in the weldment of the steel plates and those generated from the Finite Element Model Simulation were determined and tabulated.

v. A correlation between experimental and predicted values of residual stress was successfully established.

vi. Based on this, it can be concluded that Finite Element Model can efficiently be used to replicate and determine the expected residual stresses that would be generated before the actual weld is carried out.

5.2 Recommendation

The following recommendations can be noted in order to improve the results quality and make the simulation processapplicable for industrial use:

i. In order to save time, a higher version of ANSYS Multiphysics can be used for the simulationand a computer system with a higher processing capacity and also command script can be used.

ii. The welding speed of the filler metal was kept constant in this simulation, but it is very difficult to attain this in real life manual welding processes. Future research should put that into consideration.

iii. For the ease of simulation, the filler metal and the parent metals were treated as having the same material properties. But in the physical welding process, they don't and the electrode would naturally have a lower melting point than the parent metal. This can be considered in future to obtain more accurate results.

iv. It could consider different process parameters, for example welding speed, number and sequence of passes, filling material supplying, etc. Moreover, various geometrical constraints and material properties can be varied in the simulation.

v. This method implemented in welding simulation can be used in engineering processes like fluid mechanics, electromagnetic, structural and mechanical analysis.

References

Abu, M. (2013). Finite Element Analysis of Residual Stress in Welded Thick Plates of single V butt weld with different bevel angles, *University of Technology*, Petronas

American metallurgical consultants, (2012). Welding Distortion, *Welding Journal*, p.174

American Welding Society-AWS. (2001). *Specification for Carbon Steel Electrodes and Rods for Gas Shielded Arc Welding*, A5.18

Andrés, A. (2008).Finite element modelling of welded joints, *Journal of Mechanical Computation*, Vol 27, p.1445-1470

Andrea, C., Paolo, F. (2009). Multipurpose ANSYS FE procedure for welding processessimulation, *Fusion Engineering and Design*, 84. 546–553.

ANSYS V14 by ANSYS,Inc.

Bonifaz, E.(2000). Finite Element Analysis Of Heat Flow In Single-Pass Arc Welds Welding,*Research Supplement journal*, May,P 121-125.

Chang, P., and Teng, T. (2004). Numerical and experimental investigations on the residual stress of Butt welded joints, *computational material*, Vol 29, pp 511-522.

Cook, E., Johnson, D., Matti, J. and Zemmels, I. (2006). Methods of sample preparation and x-ray diffraction data analysis,*X-Ray Mineralogy Laboratory, Deep Sea Drilling Project*, University of California, Riverside

Cook, R. (1995). Finite Element Modelling for Stress Analysis, *Advanced Mechanics of Materials-2nd Edition*, John Wiley and Sons, Inc., USA.

Cronje, M. (2005).Finite Element Modelling of Shielded Metal Arc Welding, M.sc Thesis, Department of Mechanical engineering, *Stellenbosch University*, South africa.

Curtis-Wright corporation (2009).*Shot Peening Applications*.

David, R (2001): Finite Element Analysis, M.sc Thesis, Submitted to the department of Mechanical engineering, Massachusetts Institute of Technology, Cambridge, MA 02139

Dean, D. and Hidekazu, M. (2008). Prediction of welding distortion and residual stress in a thin plate butt-welded joint, *Computational Materials Science* 43, p353–365.

Deo, M., Michaleris,P. and Sun, J. (2002).Prediction of Buckling Distortion of Welded Structures, *Science and Technology Journal of Welding and Joining*, p121

Fanous, Z., Wifi, S. And Younan, A. (2003) 3-D Finite Element Modeling of the Welding Process Using Element Birth and Element Movement Techniques*, Journal of Pressure Vessel Technology*, 125, 144-150.

Fitzpatrick, M., Fry, A., Holdway, F., Kandil, F., Shackleton, J. and Souminen, L. (2005). Determination of Residual stresses by X-ray diffraction - issue 2, Open University, National Physical Laboratory, Qinetiq, Manchester materials science centre, Stresstech OY.

Goldak, J., Bibby, M., Moore, J., House, R. and Patel, B. (1986).ComputerModeling of Heat Flow in Welds, *Metallurgical Transactions B*, vol. 17B,.p 587-600.

Goldak, J., Chakravarti, A. and Bibby, M. (1984). A new finite element model for welding heat source, *Metallurgical transactions B*, 15B, 299-305.

Goodheart-Willcox Co., Inc (2011): Welding Technology Fundamentals Instructors Manual, *ISBN-13:978-1-60525-258-2, ISBN: 1-60525-258-1*.

Gurinder, S. (2013). Finite element simulation of residual stresses in butt welding of two AISI 304 stainless steel plates, *International journal on theoretical and applied research in mechanical engineering*, ISSN:2319-3182, volume 2, issue 1, 75.

Hasan, Y. (2009). Determination of Residual Stress State in Steel Weldments, M.sc thesis submitted to *The Graduate School of Natural and Applied Sciences*, Middle East Technical University.

Harshal, K. (2012): Finite element model to predict residual stresses in MIG welding, *International journal of mechanical engineering and technology (IJMET)* ISSN 0976 – 6359 (Online) Volume 3, Issue 3, September - December, pp. 350-361

Heinze, C., Schwenk, C. and Rethmeier, M. (2012). Numerical calculation of residual stress development of multi-pass gas metal arc welding under high restraint conditions.*Materials and Design* 35.p201–209

Hilley, E. (1971).Residual Stress Measurement by XRay Diffraction*,* SAE J784a, *Society of Automotive Engineers*, Warrendale, PA, p 20

Howard, K., Lawson, S. and Zhou, Y. (2006), Welding Aluminium Sheet Using A High-Power Diode Laser, *Welding Journal*, p101-110.

International Atomic Energy Agency (2003). Measurement of Residual Stress in Materials using Neutrons, *Proceedings of a technical meeting held in vienna*, IAEA-Physics Section

James, M. and Cohen, J. (1978). Measurement of residual stresses by X-ray diffraction techniques, Submitted to North western University, Department of material science, Illinois, U.S.A

Jeyakumar, M., Christopher, T., Narayanan, R. and Nageswara, B. (2013): Residual Stress Evaluation in Butt-welded IN718 Plates.*Canadian Journal of Basic and Applied Science*, Vol. (01) - september - issue 02 (2013) 88-99

Jeyakumar, M., Christopher, T., Narayanan, R. and Nageswara, B. (2013).Residual Stress Evaluation in Butt-welded joint of ASTM A36 Steel Plates,*International Journal of Electronics Communication and Computer Engineering*, Volume 4, Issue 2, ISSN (Online): 2249–071X, ISSN (Print): 2278–4209

Keil, S.(1992).Experimental Determination of Residual Stresses with the Ring-Core Method and an Online Measuring System, *ExperimentalTechniques,*Vol.16, No. 5, pp.17-24.

ManGyun, N. (2007): Predictionof residual stress for dissimilar metals welding atNuclear power plants using fuzzy neural network models, *Nuclear Engineering and Technology Journal*, vol. 39, no. 4, p337-348

Michaleris, P. and DeBiccari, A. (1986). Prediction of Welding Distortion, *Welding Journal*, 76(4). p172-180

Naeem, D. (2009). Analysis of weld-induced residual stresses and distortions in thin-walled cylinders, *Journal of Mechanical Science and Technology* (23). p1118-1131

National Steel Raw Materials Exploration Agency, Kaduna

Nguyen, T. (2004). Thermal Analysis of Welds, *WIT Press*, Southampton, UK.

Paul, S. (2003): X-Ray DiffractionResidual Stress Techniques, *Metals Handbook*. 10. Metals Park, American Society for Metals, 1986, 380-392.

Radaj, D (2003). Welding Residual Stresses and Distortion,Calculation and Measurement, *Springer-Verlag*, Berlin.

Rosenthal, D (1946).The Theory of Moving Sources of Heat and its Application to Metal Treatments, *Trans ASME*, 68. p849-865.

Rossinia, N., Dassistia, M., Benyounis, Y. and Olabi, G. (2007). Methods of Measuring Residual Stresses in Components, *Materials and Design* .28: 2295- 2302

Satish, D. (2001).Residual Stress Measurement and Analysis by Destructive and Non Destructive Techniques.

Shimadzu corporation. (2007). *XRD-6000 operation manual*,

Stamenkovic, D. and Ivana, V. (2009). Finite Element Analysis of Residual Stress in Butt Welding Two Similar Plates, *Scientific Technical Review*, Vol 511, No. 1, page 57-60

Weaver, M. (1999). Determination of Weld Loads and Throat Requirements using Finite Element Analysis with Shell Element Models - A Comparison with Classical Analysis, *Welding Journal v78*, n. p 116-126

Withers, P. and Bhadeshia, H. (2001). Residual stressMeasurement techniques, *Material Science and technology*, Vol. 17, p 355-365

http://www.amfiller.com/catalog.html/low_alloy_electrodes, accessed on 21st April, 2014.

http://www.myweb.ncku.edu.tw/~hhlee/Myweb_at_NCKU/ANSYS14.html, accessed on 3rd June, 2013.

http://www.onealsteel.com/carbon-steel-plate-a36.html, accessed on 19th January,2014.

http://www.residualstress.org, accessed on 11th November, 2013.

http://www.weldingweb.com/smmawm/pic.html, accessed on 30th December,2013.

http://www.amfiller.com/catalog.html/flux_cored_wires, accessed on 21st April, 2014.

http://www.navybmr.com/studymaterial/14250a/14250A_ch8.pdf, accessed on 10th Octeber,2015

Xu, S. (2010).Modeling residual stresses and deformation in metal at different scales, Ph.D. Thesis, submitted to *University of Oxford*,